Doctoral Thesis

Development of Statistical Geometric Models

for a Driver's Hip & Eye Location and

Identification of Sitting Strategies for Driving Postures

Jangwoon Park (박 장 운)

Division of Mechanical and Industrial Engineering

Pohang University of Science and Technology

2013

운전자 엉덩 관절과 눈 위치 추정을 위한
통계적 기하학적 모형 개발 및 착좌 유형 분류

Development of Statistical Geometric Models
for a Driver's Hip & Eye Location and
Identification of Sitting Strategies for Driving Postures

ABSTRACT

Drivers' hip locations (HLs), eye locations (ELs), and sitting strategies have been used as reference data to design an ergonomics automobile interior. HL is a 2D coordinate which represents a pivot point between the torso and upper leg of a driver in sagittal plane, and the distribution of HLs is used to determine the adjustment range of driver seat. On the other hand, EL is a 2D coordinate which represents a driver's eye location in a sagittal plane, the distribution of ELs (eyellipse) is used to determine the locations of displays, mirrors, and the height of windshield in clear visibility aspect. Lastly, the sitting strategies are classes of drivers' preferred driving postures which can be used as reference data to create a humanoid's driving posture in a virtual automobile design/evaluation process.

Although many prediction models to predict a driver's HL and EL have been developed, the existing models have limitations. First, the existing prediction models have low prediction accuracies. Second, the information of prediction accuracy (adj. R^2 and $RMSE$) was not provided clearly.

Meanwhile, a preferred driving posture is needed to build up a humanoid's posture in a virtual environment, a few several studies have been conducted for drivers' sitting strategies. Moreover, they did not analyze a gender and OPL effect to the sitting strategies. In addition, the classification method of driving posture is subjective, not objective.

The objectives of the present study are (1) development of new prediction models for a driver's HL and EL, and evaluation of the effectiveness of developed models, (2) identification of sitting strategies which statistically represent drivers' preferred driving

postures and an analysis of related effects to the sitting strategies, lastly (3) validation of the identified sitting strategies based on field observations.

The present study measured 20 male and 20 female drivers' driving postures in 3 occupant package layout (OPL) conditions (coupe, sedan, and SUV) using a motion capture system. Measured postures were reconstructed by digital human models (humanoids) in a 3D virtual environment using RAMSIS® and the participants' HLs, ELs, and joint angles were extracted from the humanoids. The new prediction models (statistical geometric models, SGMs) were developed by statistical analysis (multiple regression analysis) based on geometric equations of participants' anthropometric dimensions and joint angles for their HLs and ELs. Next, the sitting strategies were classified by cluster analysis; next, gender and OPL effects to the sitting strategies were statistically identified.

The developed SGMs can be used as effective package design tools because they show higher prediction accuracies than the existing models. The average adj. R^2 of SGMs is 1.1 ~ 3.7 times higher than Reed et al. (2002)'s models and root mean squared error (*RMSE*) of SGMs is 1.7 ~ 1.8 times smaller than Reed et al.'s models. Moreover, *RMSE* of the developed SGMs in difference OPL conditions (coupe, sedan, and SUV) are 1.7 ~ 4.3 times smaller than the Reed et al.'s models. These results indicate that the prediction accuracies of SGMs are more stable than the Reed et al.'s models in different OPL conditions.

The sitting strategies of driving postures were statistically classified into 3 types of driving posture for upper-body (slouched, erect, and reclined posture) and 3 types for lower-body (knee bent, knee extended, and upper-leg lifted). The classified driving postures for upper-body were significantly affected by a driver's gender ($\chi^2(2) = 8.0$, $p = .02$). For example, in the reclined sitting strategy group, there are 36.2% of males and 15.3% of females. However, in the erect sitting strategy group, there are 24.1% of males and 42.4% of females. The classified driving postures for lower-body were significantly affected by OPL conditions ($\chi^2(4) = 56.3$, $p < .01$). For example, 84.2% of knee bent strategy was appeared in SUV condition, however there is only 2.6% of knee bent posture was appeared in coupe condition.

Field based driving postures were collected to validate the identified sitting strategies in lab test. The present study proposed image based driving posture analysis protocol and constructed driving posture database for 214 Korean drivers (117 males and 107 females). As a result of validation study, the frequencies of the lab based and field based sitting strategies (slouched, erect, and reclined) in each 3 OPL conditions (coupe, sedan, and SUV) show no significant differences of their homogeneity ($p = 39$ for coupe, $p = .78$ for sedan, and $p = .37$ for SUV).

The developed SGMs and identified sitting strategies have high applicability as reference data to design an ergonomics automobile interior such as seat adjustment range and windshield height for a new design of automobile package.

TABLE OF CONTENTS

LIST OF FIGURES

LIST OF TABLES

Chapter 1   INTRODUCTION

1.1. Problem statement

Drivers' hip locations (HLs), eye locations (ELs), and sitting strategies can be used as reference data for an ergonomics driver seat design in terms of accommodation, reach, visibility, comfort, safety, performance, convenience, and clearance. HL is a 2D coordinate which represents a pivot point between the torso and upper leg of a driver, and the distribution of HLs collected from thousands of drivers is used to determine the adjustment range of seat (Parkinson et al., 2005, 2007; Philippart et al., 1984). On the other hand, EL is a 2D coordinate which represents a driver's eye location, the distribution of ELs (eyellipse) is used to determine the locations of viewing components such as displays, mirrors, and windshields (Bhise, 2011; SAE J941, 2010). Lastly, the sitting strategies are classes of preferred driving postures which can be used as reference data to build-up a digital human models' driving postures in a virtual automobile design/evaluation process (Park, 2006).
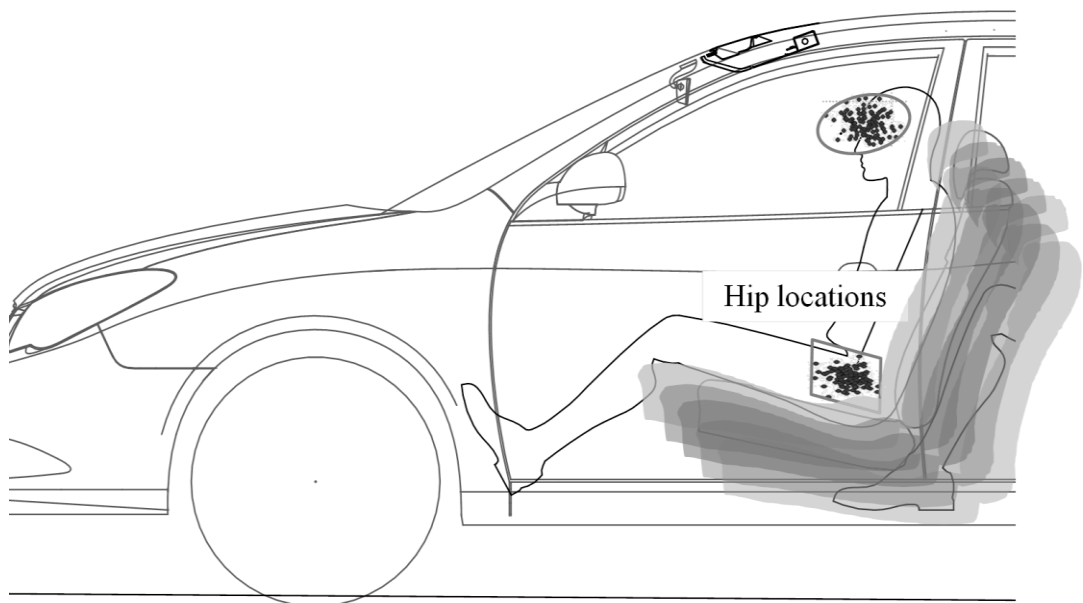
Figure 1.1. Reference data for automobile ergonomics: drivers' hip & eye locations

To predict drivers' HLs and ELs, a few geometric or statistical models have been developed. As shown in Figure 1.2, Driffrient et al. (1981) developed a geometric model to predict a horizontal distance from a driver's ankle to HL (Hip_x reankle) using the driver's lower-body link lengths (femoral link and shank link lengths) and related joint angles (hip and knee angles). On the other hand, Society of Automobile Engineers (SAE) suggested statistical models to predict a driver's HL and EL based on the linear relationship between occupant package layout (OPL) dimensions such as seat height (H30) and steering wheel location from a pedal. As shown in table 1.1, SAE J1517 (2011) suggested horizontal HL (Hip_x) prediction models for each stature groups (2.5^{th}, 5th, 10th, 50th, 90th, 95th, and 97.5^{th} %ile) based on H30 and square of H30. Moreover, SAE J941 (2010) suggested horizontal EL (Eye_x) and vertical EL (Eye_z) prediction models using OPL variables (e.g., steering wheel height and pedal location). Lastly, Reed et al. (2002) developed statistical HL and EL prediction models using driver's anthropometric variables (stature and sitting height/stature), OPL variable (horizontal location of steering wheel from BOF), and seat configuration variables (seat height and cushion angle) as shown in Figure 1.3.
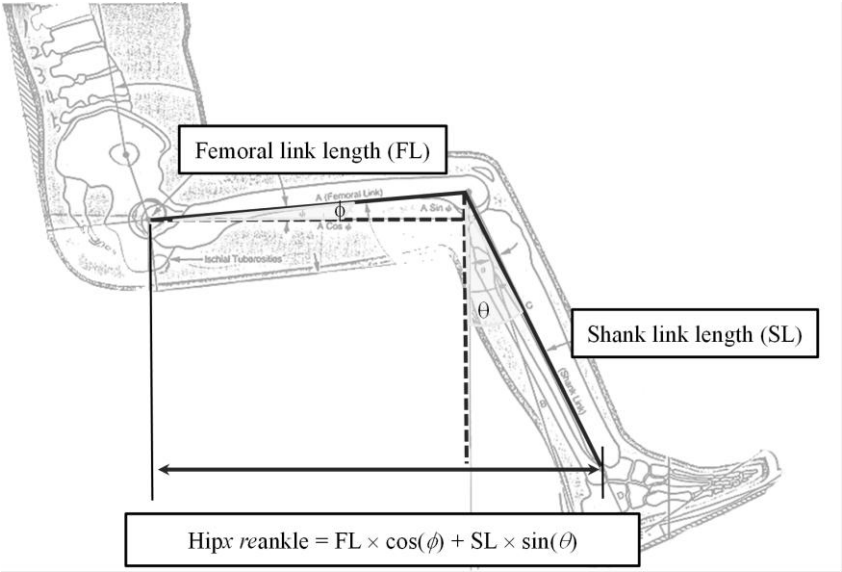
Figure 1.2. Prediction model of horizontal HL using link lengths and joint angles (Diffrient et al., 1981)

Table 1.1. Summary of HL and EL prediction models (unit: mm)

Dependent variable	SAE model (SAE J1517 for HL; SAE J941 for EL)	Reed et al.(2002)		
		Model	Adj. R^2	RMSE
Hip$_x$	$x_{2.5}$: $687.1 + 0.895 \times H30 - 0.002 \times H30^2$ x_5 : $692.6 + 0.981 \times H30 - 0.002 \times H30^2$ x_{10} : $715.9 + 0.969 \times H30 - 0.002 \times H30^2$ x_{50} : $793.7 + 0.903 \times H30 - 0.002 \times H30^2$ x_{90} : $885.0 + 0.739 \times H30 - 0.002 \times H30^2$ x_{95} : $913.7 + 0.572 \times H30 - 0.002 \times H30^2$ $x_{97.5}$: $936.6 + 0.613 \times H30 - 0.002 \times H30^2$	$84.8 + 0.4659 \times$stature $- 430.1 \times$sitting height/stature $- 0.1732 \times H30$ $+ 0.4479 \times$SWtoBOFx $- 1.04 \times$cushion angle (°)	0.78	35.9
Eye$_x$	L1 + 664 + 0.587×L6 − 0.176×H30 − 12.5×t	Eye$_x$ reHip = -916.0 + 0.1187×stature + 1347.2×sitting height/stature + 0.1563×SWtoBOFx + 1.15×cushion angle (°)	0.23	41.7
		Eye$_x$ reBOF = -836.6 + 0.5842×stature + 916.6×sitting height/stature − 0.1559×H30 + 0.6101×SWtoBOFx	0.71	50.9
Eye$_z$	H8 + 638 + H30	Eye$_z$ reHip = -261.5 0.3336×stature + 675.8×sitting height/stature −0.0544×SWtoBOFx	0.72	22.9
		Eye$_z$ reAHP = -267.1 + 0.3122×stature + 679.9×sitting height/stature + 1.0319×H30 + 0.0292×SWtoBOFx	0.89	21.8

Notes: Hip$_x$ = horizontal hip location from the origin (projected point from the center of accelerator pedal to the floor); Eye$_x$ = horizontal eye location; Eye$_z$ = vertical eye location; AHP = accelerator heel point; BOF = ball of foot; H8 = AHP z coordinate; H30 = seat height; PRP = pedal reference point; L1 = horizontal PRP; SW = steering wheel; L6 = horizontal distance from the center of SW to PRP; t = transmission type (1 with clutch pedal, 0 without clutch pedal).
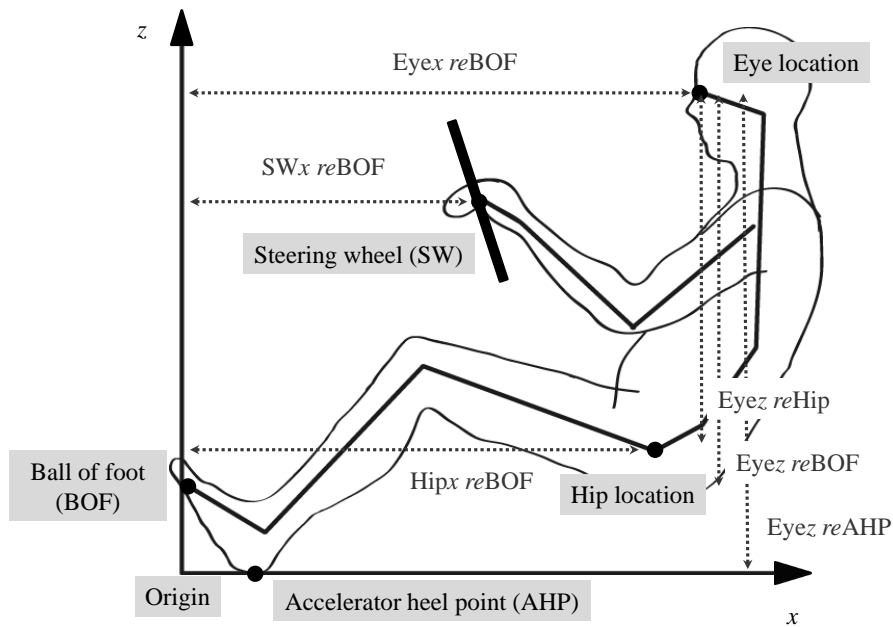
Figure 1.3. Dependent variables of Reed et al.'s models and design reference points

Although many geometric models have been developed to predict a driver's HL and EL, they have a limitation to apply in an automobile design industry. The geometric model for HL and EL, they used link lengths which are anatomical lengths, not measurable lengths. For example, a driver's shank link length is a distance from ankle to knee joint; however, the ankle and knee joint locations are hard to find precisely from the driver's skin. Generally, a driver's body sizes were measured by Martin's anthropometer based on the skin surface landmarks (Chaffin et al., 2006). However, the femoral link and shank link lengths of Diffrient et al. (1981)'s Hip_x reankle model are anatomical lengths, and they can't be measured by Martin's anthropometer.

The existing statistical HL and EL prediction models based on the linear relationship between driver's anthropometric variables and OPL variables have a limitation of prediction accuracy. SAE J1517's HL prediction model was developed by considering a seat height as an independent variable and SAE J941's EL prediction model was considered the simple statistical linear relationship between OPL variables such as seat

4

height and steering wheel location; however, they didn't considered a driver's human variables such as the driver's anthropometric dimensions and driving postures. Also, Reed et al.'s models were only considered the statistical linear relationship between a driver's anthropometric variables (e.g., stature and sitting height/stature) and OPL variables (e.g., H30 and cushion angle); however, there are no driving posture variables.

Meanwhile, many researches were conducted to identify the sitting strategies (statistically represent preferred driving posture classes) for an efficient evaluation of an automobile interior. Park (2006) identified 5 sitting strategies through cluster analysis based on 126 Korean male drivers' driving posture data (knee, hip, shoulder, and elbow angle). Andreoni et al. (2002) identified the 3 upper-body sitting strategies (dorsal scapular, dorsal, and lumbar strategy) and 3 lower-body sitting strategies (ischiatic, intermediate, and trochanteric strategy) based on the visual observation of seating pressure images for 8 males.

First
32.5%

Second
23%

Third
20.5%

Fourth
12%, 12%
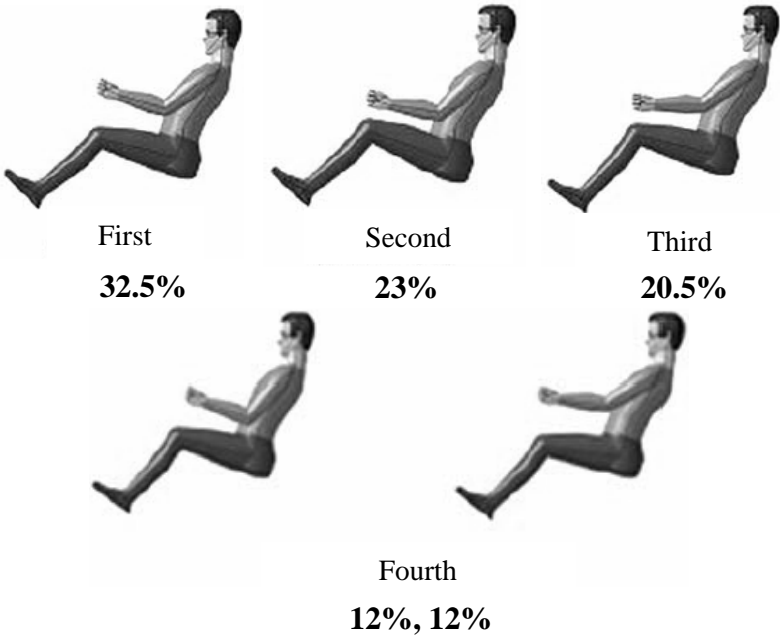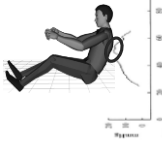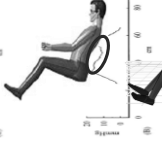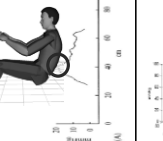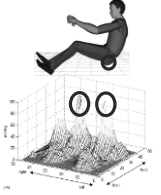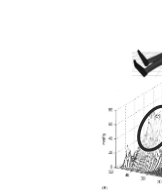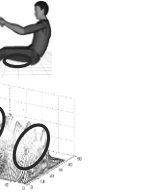
Figure 1.4. Identification of sitting strategies based on the posture data analysis

(Park, 2006)

Table 1.2. Identification of sitting strategies based on the seating pressure observation (Andreoni et al., 2002)

	Sitting strategy					
	Seatback			Seatpan		
	Dorsal Scapular	Dorsal	Lumbar	Ischiatic	Intermediate	Trochanteric
Pressure distribution						
% of drivers	38%	50%	12%	63%	12%	25%

Although the sitting strategies were identified by two quantitative data sets (driving posture and seating pressure), the identification method of sitting strategies was not quantitative and the factors to affect the sitting strategies such as OPL condition and gender were not analyzed clearly. Andreoni et al. (2002)'s visual observation based sitting strategy identification method has a limitation due to lack of objectiveness for a visual observation of seating pressure distributions. Park (2006) identified sitting strategies based on cluster analysis of 126 male drivers' 4 joint angles (shoulder, elbow, knee, and hip angles); however, Park didn't analyze the factors (e.g., driver's gender and OPL condition) to affect the sitting strategies, so that the identified sitting strategies are hard to apply in various automobile package designs.

1.2. Objectives of the study

The present study has 3 research objectives: (1) development and evaluation of statistical geometric models for a driver's HL and EL, (2) identification of sitting strategies and related factors based on an objective method, and (3) validation of the identified sitting strategies based on the field observations).
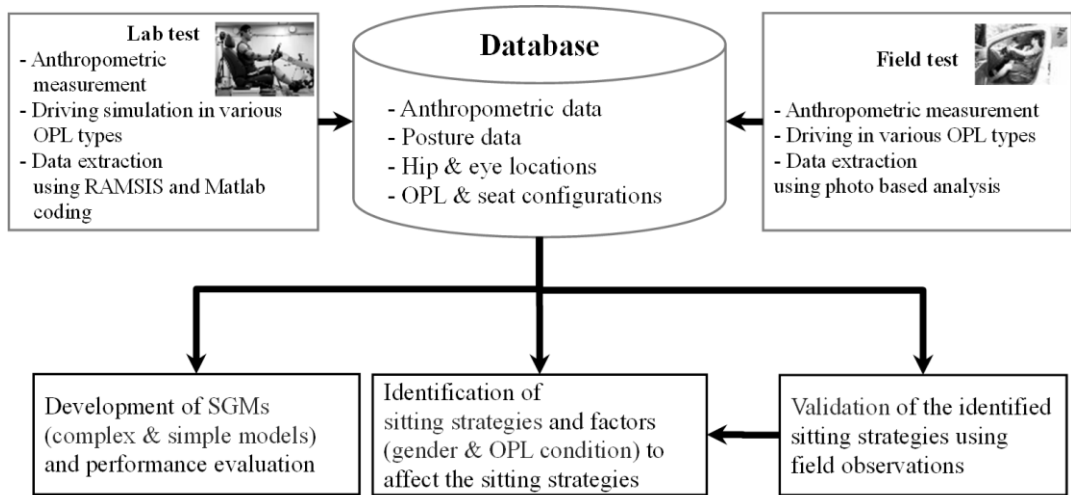
Figure 1.5. Research framework of the present study

First, the present study will develop and evaluate statistical geometric models to predict a driver's HL and EL based on the geometric relationship between drivers' anthropometric dimensions, joint angles, and hip & eye locations. The existing models (Diffrient et al., 1981; Reed et al., 2002; SAE J1517, 2011; SAE J941, 2010) used a driver's link length which cannot be measured precisely. Moreover, they didn't consider driving posture variables because the existing models were considered the statistical linear relationship between a driver's anthropometric dimensions and OPL conditions only. However, the present study will develop novel models (statistical geometric models, SGMs) to predict a driver's HL and EL by considering the statistical & geometric relationship of a driver's body sizes and driving postures. Meanwhile, the present study will evaluate the performances of SGMs by comparing the performances of existing models (Reed et al., 2002; SAE J1517, 2011; SAE J941, 2010) in terms of the prediction accuracy and stability. For example, the prediction accuracy of the SGMs and Reed et al.'s models can be evaluated by adj. R^2 and *RMSE* for each of models. Next, the prediction stability can be evaluated by comparing *RMSEs* of SGMs and Reed et al.'s models for difference OPL conditions (coupe, sedan, and SUV).

Second, the present study will systematically identify the sitting strategies. The sitting strategy which statistically represents a preferred driving posture can be used as reference data in an automobile interior design. The present study will supplement the limitations (not quantitative method, no interpretation of the classified sitting strategies) of the previous sitting strategy researches.

Lastly, the present study will validate the lab test based sitting strategies using field observations. The validation method is consist of 4 stages: (1) taking photos of driving postures in various OPL conditions using a digital single lens reflex (DSLR) camera, (2) developing a driving posture extraction protocol from the driving posture image, (3) establishing the field based driving posture database, and (4) statistically evaluating the homogeneity of the ratios for lab and field based sitting strategies in certain OPL condition.

1.3. Significance of the study

In an academic aspect, the SGMs will have higher prediction accuracy, and higher prediction stability than existing models. The previous statistical models were developed based on the simple statistical linear relationship between a driver's anthropometric and OPL variables without considering a driver's posture variables, so that the prediction accuracies of the existing models seem to be low (e.g., adj. R^2 of the Reed et al.'s model for Eye_x reHip = 0.23). Moreover, the Reed et al.'s models used OPL variables (e.g., seat height and cushion angle) as independent variables, so that the prediction stability of Reed et al.'s models in different OPL conditions seems to vary largely. However, the SGMs will be developed based on the statistical & geometrical relationship between driver's anthropometric variables and posture variables, so that their prediction performance will not be affected in any OPL conditions, so that the prediction stability of SGMs in difference OPL conditions will better than the Reed et al.'s models.

In a practical aspect, the identified drivers' sitting strategies and related factors which can be used as reference information in an automobile design process. Sitting strategy can be used as reference information to build a humanoid's driving posture in virtual

environment to evaluate an automobile interior in an early design stage. However, Andreoni et al.'s identification method is somewhat qualitative (not quantitative), so that the reliability and applicability of Andreoni et al.'s sitting strategies seem to be low. Moreover, the factors to affect the sitting strategies were not clearly analyzed yet. The present study will find the factors to affect a driver's sitting strategy clearly to apply the sitting strategy in an automobile design stage efficiently and effectively.

Lastly, the developed SGMs and identified sitting strategies can be effectively synchronized to improve effectiveness and efficiency of OPL design/evaluation process. For example, 5th %ile and 95th %ile of drivers' HL and EL can be effectively predicted using the SGMs and the sitting strategies, so that this HL and EL prediction process can reduce the design/evaluation time of an automobile interior.

1.4. Organization of the Dissertation

The remainder of this dissertation is organized into eight chapters and five appendices. Chapter 2 describes literatures about drivers' HLs, ELs and sitting strategies. Chapter 3 describes the development of SGMs to predict various drivers' HLs and ELs. Chapter 4 describes the comparison of the SGMs and Reed et al.'s models in terms of prediction accuracy. Chapter 5 describes the identification of sitting strategies and related factors based on the measured postures in a lab test. Chapter 6 describes the validation study of the identified sitting strategies with large samples of driving postures in field. Chapter 7 describes the discussion about the values and applications of this study, and lastly chapter 8 describes the conclusion of this study.

Chapter 2   LITERATURE REVIEW

2.1. Occupant packaging

Occupant packaging is a design process of an automobile interior by considering drivers'
accommodation, clearance, comfort, reach, visibility, safety, and convenience. Many
researches about occupant packaging have been conducted since its importance was
increased. Roe (1993) emphasized an importance of drivers' functional anthropometry
which accommodate 95% of drivers' various stature (e.g., 2.5^{th}, 50th, and 97.5^{th} %ile).
Illustration of the functional anthropometry is shown at Figure 2.1, drivers' hand reach,
eye location, etc.
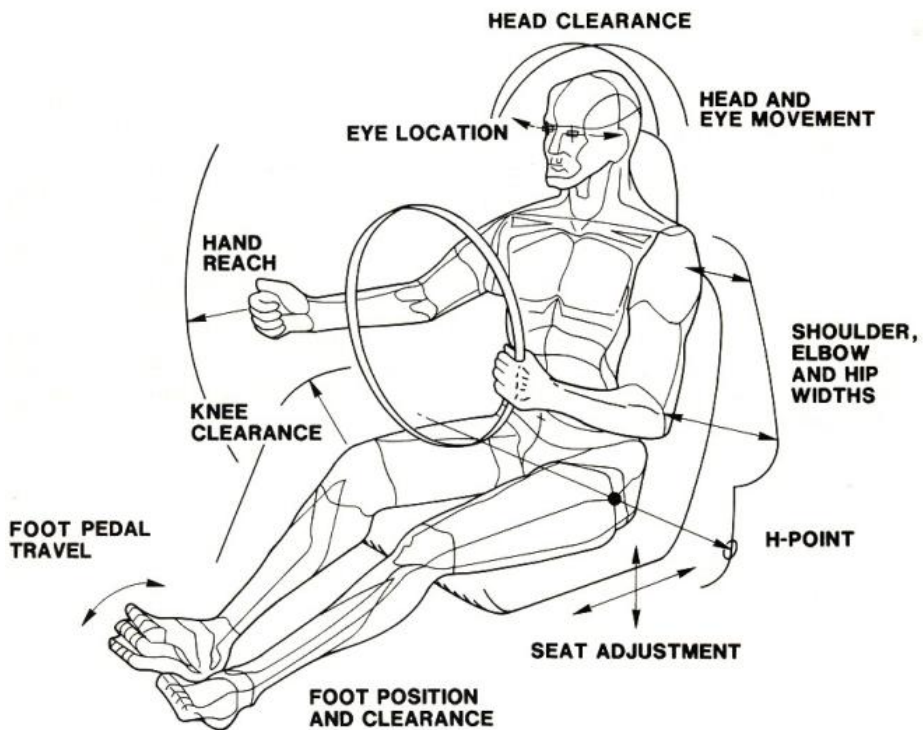
Figure 2.1. The functional anthropometry for occupant packaging (Roe, 1993)

About clearance, drivers' eyellipse, head position contour, and knee clearance were analyzed. SAE J941 (2010) provided eyellipse and head position contour range which accommodates 95% and 99% of American drivers' eye & head location (Figure 2.2). Moreover, Bhise (2011) recommended a knee clearance from knee pivot point to vehicle interior (> 51 mm) by considering a driver's pedal control task (Figure 2.3).
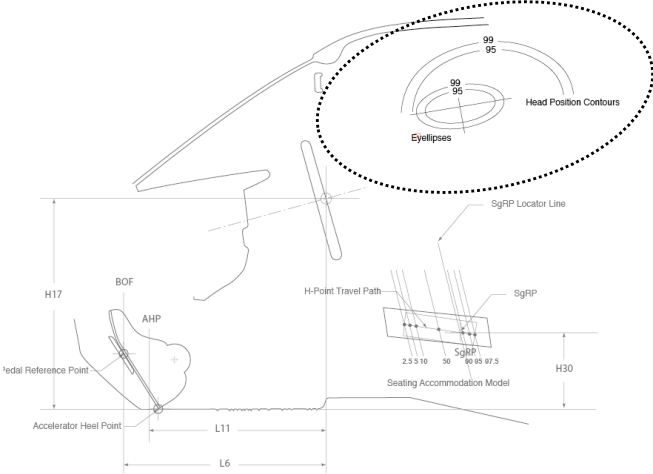
Figure 2.2. Eyellipse and head position contours of drivers (SAE J941, 2010)
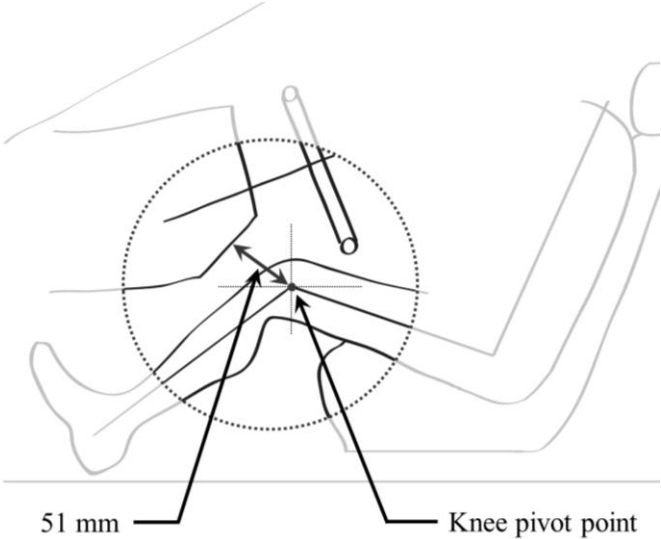
Figure 2.3. Recommended knee clearance (Bhise, 2011)

About comfort, drivers' preferred driving postures and preferred seating pressures were analyzed. Park et al. (2002) analyzed correlation between 43 drivers' body sizes, their preferred driving postures, and their preferred seating configurations as shown in Figure 2.4. For example, Park et al. reported that when the taller drivers seated in an automobile interior, the more spaces they needed beyond from a steering wheel (correlation coefficient of a driver's stature and seat position = 0.583, $p < .001$). Mergl et al. (2005) quantitatively analyzed body pressure ratio (BPR) of drivers' preferred upper- & lower-body seating pressures. BPR is a quantitative measure for analysis of seating pressure distribution which can be divided into 9 body parts for upper-body pressures, 8 body parts for lower-body pressures based on the driver's anthropometric information such as back length, hip breadth (Figure 2.5); and certain body part area's seating pressure ratio (%) can be calculated from the upper-/lower-body's total seating pressure.
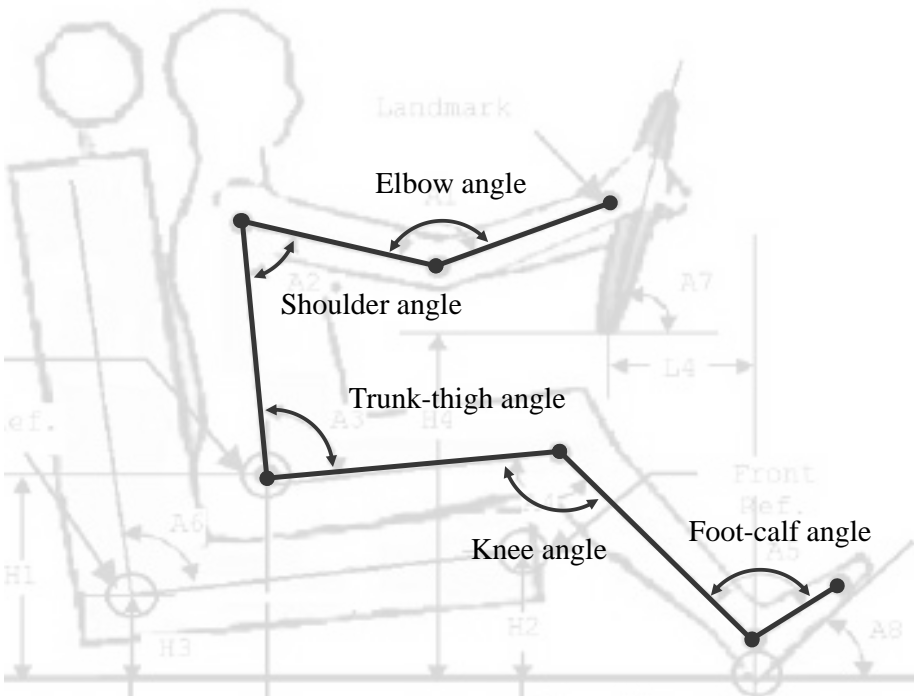
Figure 2.4. Selected joint angles to analyze a driver's driving posture (Park et al., 2002)

For example, the BPR of lower-body seating pressure is the body segment pressure ratio (%) over total pressure, which was divided into 8 parts by a body grid which was generated using the driver's hip breadth and upper-leg length. Meanwhile, Mergl et al. (2005) analyzed the relationship between body segment pressure distribution and discomfort, so that Mergl et al. reported that there is nonlinear relationship between hip pressure and subjective discomfort as shown in Figure 2.6.
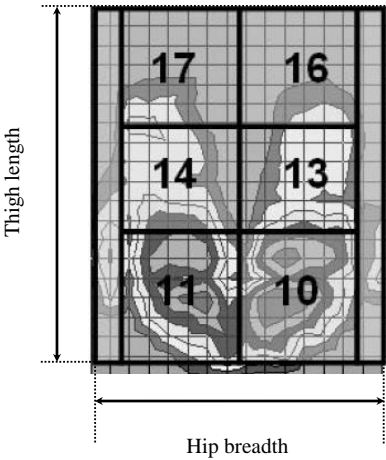
Figure 2.5. The body pressure ratio analysis for lower-body seating pressure
(Mergl et al., 2005)
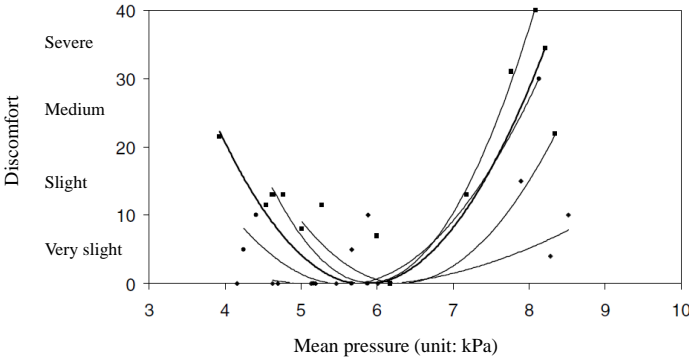
Figure 2.6. Nonlinear relationship between hip pressure and discomfort
(Mergl et al., 2005)

About reach, drivers' forward reach envelopes have been analyzed. SAE J287 (2007) analyzed US drivers' maximum hand reach envelope, the reach envelopes were identified that participants were asked to comfortably grasp a knob as much as forward they can with three fingers (Figure 2.7). Meanwhile, SAE J827 provided tables that present horizontal distances forward from hand reach reference plane (Figure 2.8) and suggested the prediction model for the location of hand reach reference plane (Equation 2.1).
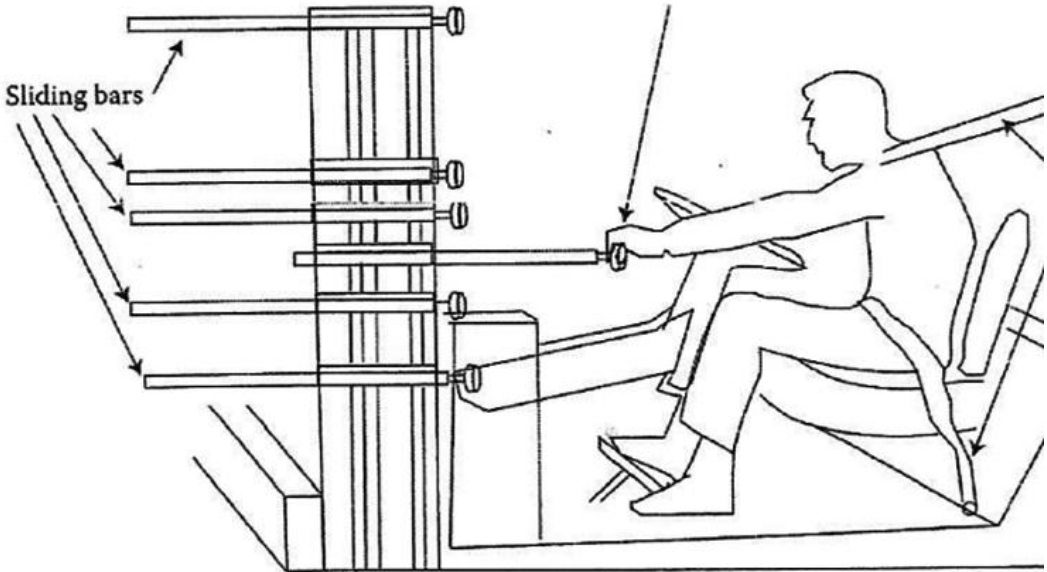
Figure 2.7. An analysis of driver reaches using knob in seating buck (Bhise, 2011)
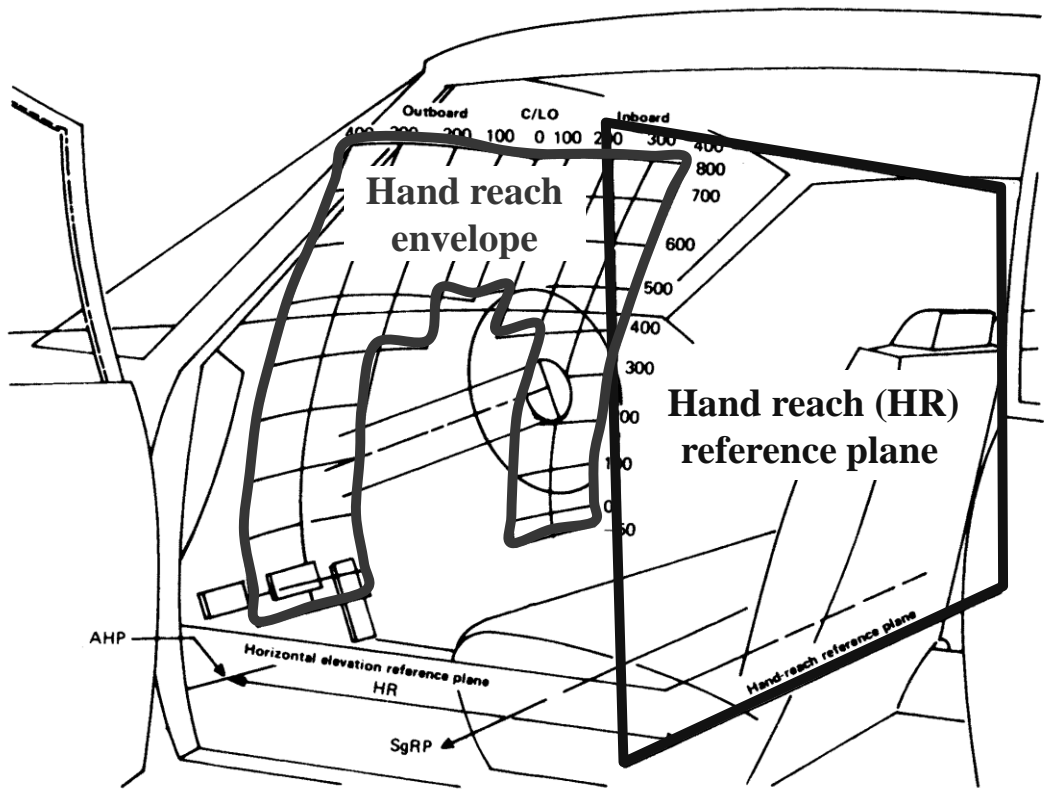
Figure 2.8. Hand reach envelope from the hand reach reference plane (SAE J287, 2007)

$$HR = 786 - 99 \times G \qquad \qquad \text{Equation 2.1}$$
$$G = 0.00327 \times H30 + 0.00285 \times H17 - 3.21$$

where: HR = hand reach,
          G = general package factor,
          H30 = seat height,
          H17 = height of the center of the steering wheel

About visibility, drivers' visible areas were analyzed using drivers' eyellipse. SAE J941 (2010) suggested 95% of driver's visible area using the tangent line (cutoff line) using US drivers' 2D eyellipse (74% US drivers' eye locations were inclusive) as shown in Figure 2.9.
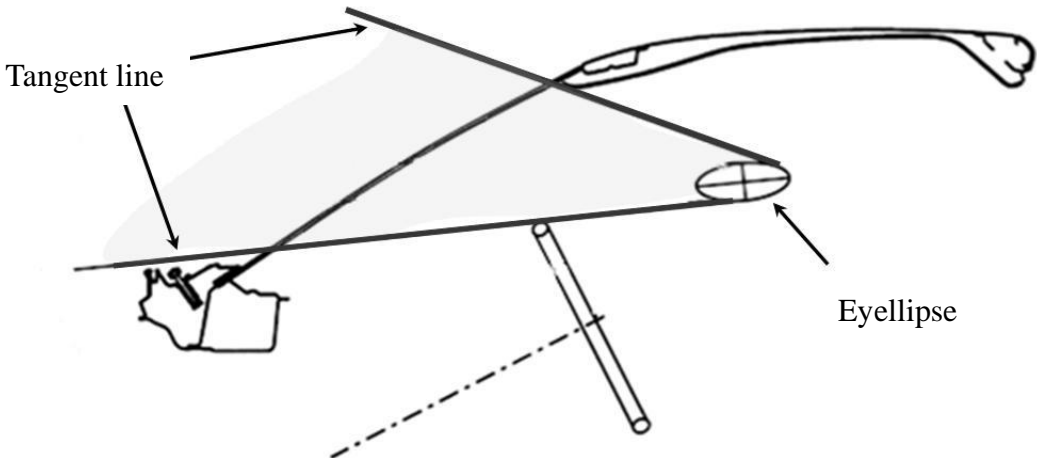
Figure 2.9. Drivers' visible area analysis using the tangent line of eyellipse
(SAE J941, 2010)

2.2. Design reference points

2.2.1. Hip location (HL)

HL is a 2D coordinate (x, z) which represents a driver's hip location and its distribution can be used as important reference data in an automobile design process. The coordinate of HL is identified in the 3D coordination system which was defined by SAE J1100 (2005) to increase the effectiveness of an automobile design process. As following the 3D coordinate system of SAE J1100 (Figure 2.10), x-axis means forward and backward direction (positive direction is backward of car), y-axis means left and right direction from the driver's seat, lastly z-axis means upward and downward direction (positive direction is upward of car). Meanwhile, the meanings of HL and SgRP are summarized in Table 2.1.
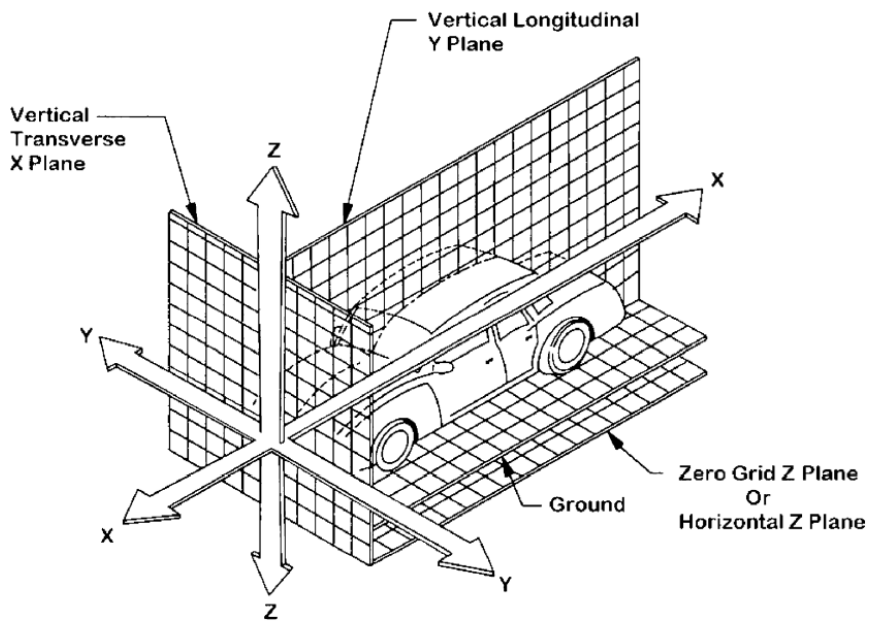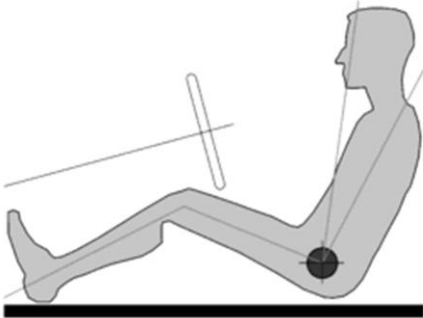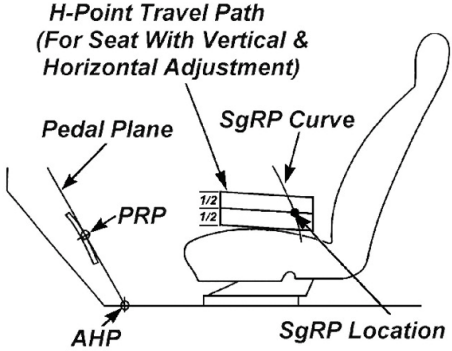
(a) 3D reference coordinate system for an automobile design
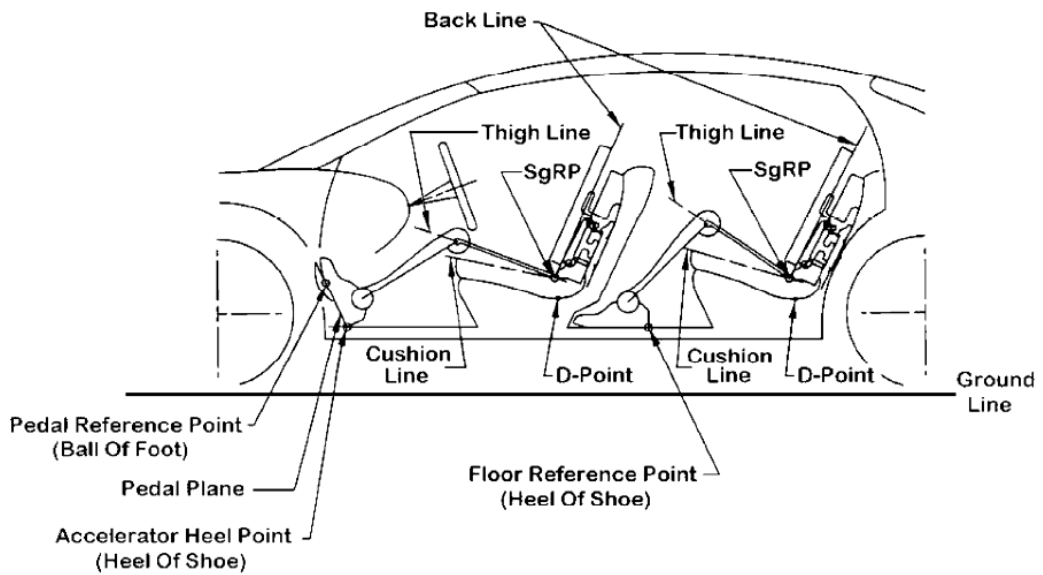
(b) Design reference points

Figure 2.10. 3D coordinate system and design reference points (SAE J1100, 2002)

Table 2.1. Definition of hip location and seating reference point

Hip location	**Seating reference point (SgRP)**
Theoretical, relative location of an occupant's hip, specifically the pivot point between the torso and upper leg portions of the body (Edsall, 2004)	Location where the SgRP curve intersects the design H-Point travel path (Roe, 1993)

For the right cell figure:

H-Point Travel Path (For Seat With Vertical & Horizontal Adjustment)

Pedal Plane

SgRP Curve

PRP

1/2
1/2

AHP

SgRP Location

SgRP Curve—The SgRP curve is positioned aft of the PRP using the following equation:

$$SgRP_x = 913.7 + 0.672316(H30) - 0.0019553(H30)^2 = \text{Distance (in mm) rearward of PRP}$$

The H-point machine (HPM) was developed to measure a driver's hip location by a standard protocol. The HPM (Figure 2.11) is a mechanical measurement tool of a driver's hip location and the HPM was used to accommodate 95% of US drivers' hip locations in an automobile design process. The HPM can adjust lengths of leg, trunk, and weight of the machine. The HPM can be seated on a certain seat configuration by following the HPM setting protocol of SAE J826 (1995). The seated HPM is used to measure the machine's hip location from the floor. Meanwhile, the defined HPM setting protocol of SAE J826 is used as a global standard to measure a hip location under the certain automobile package design.
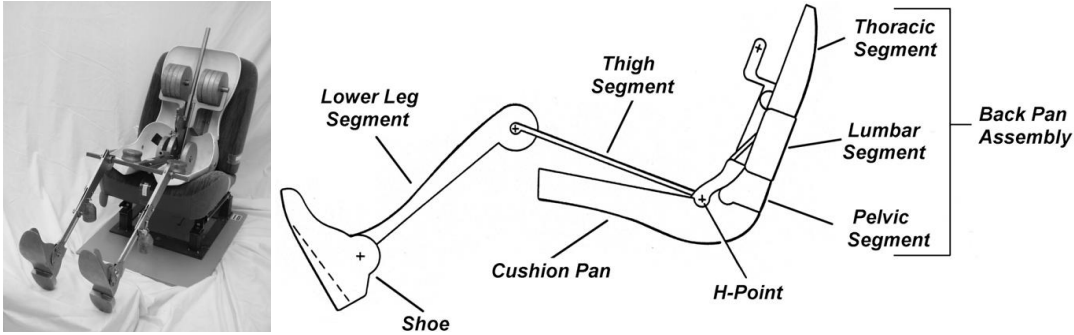
(a) Old H-point machine
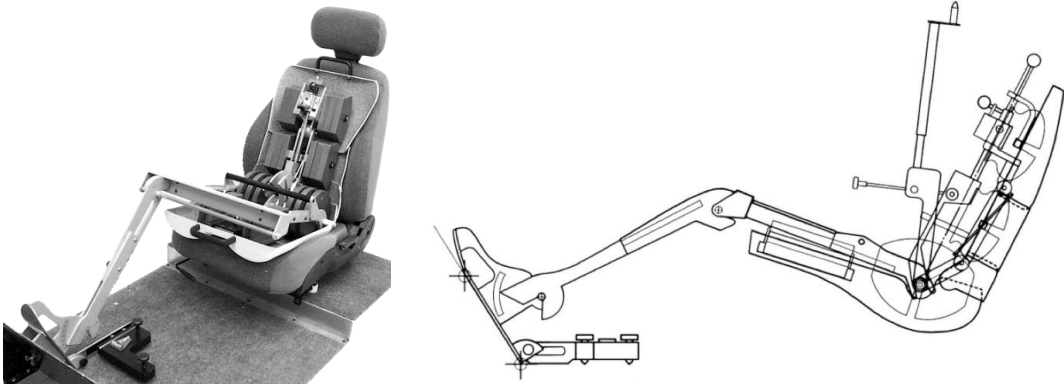
(b) New H-point machine

Figure 2.11. H-point machine to measure a US percentile driver's hip point
(SAE J826, 1995; SAE J4002, 2008)

The HL distribution covered various body sizes of drivers is used as reference data to design a seat adjustment range and steering wheel adjustment range. As shown in Figure 2.12, Parkinson et al. (2005) predict 1,774 US drivers' HLs using Reed et al.'s models through US Army anthropometric data (Gordon et al., 1988) to figure out an optimal seat adjustment range and steering wheel adjustment range. Meanwhile, SAE J4004 (2009) proposed HL accommodation ranges for various statures (80th, 90th, 95th, 97.5th, and 98th %ile) of drivers as a design guide for seat adjustment range (Figure 2.13).
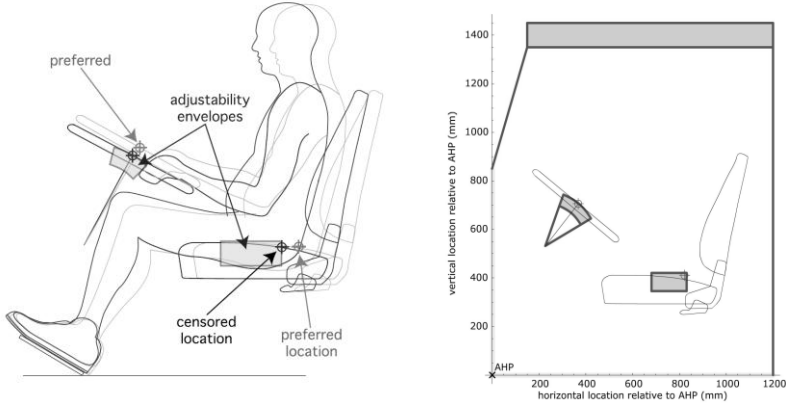
Figure 2.12. Design of adjustment ranges for a steering wheel and a seat

(Parkinson et al., 2005)
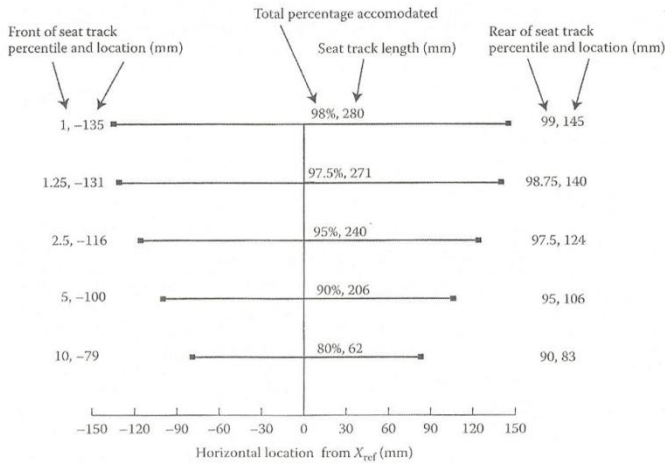
Figure 2.13. Recommended seat adjustment range based on a driver's stature percentile

(SAE J4004, 2009)

2.2.2. Eye location (EL)

EL is a coordinate to represent a driver's eye location which can be used as important reference data to create an eyellipse (reference information to design a visibility based on US driver population). Eyellipse is a terminology which combined 'eye' and 'ellipse', and it is 3D ellipsoid to statistically represent drivers' ELs (Figure 2.14). SAE J941 (2010) proposed EL prediction model to predict the centroid of US drivers' eyellipse. Meanwhile, 95% or 99% US drivers' 2D eyellipse in a side view, there are tangent cutoff line (Figure 2.15) which can be generated on the surface of the eyellipse to evaluate the 95% or 99% US drivers' visibility in a certain automobile package layout. SAE J941 proposed two dimensional sizes of the eyellipses (Table 2.2) by considering seat track lengths (1 ~ 133 mm; > 133 mm) and tangent cutoff percentiles (e.g., 95% and 99%). In addition, PDE Automotive company in Netherland invented a driver's eye location measurement system (Figure 2.16) using a HPM, IR camera, and a censor which located on the head of HPM. Reed et al. (2001) introduced the measurement device of HPM (Figure 2.17) for a driver's EL and head room. Parkinson et al. (2007) designed the windshield height of a trunk by following the design guideline of MIL STD-1472F (1999)'s safety/regulatory constraint, ground view, which means a driver must have a clear view on the floor at least 3 meter without any barrier (Figure 2.18).
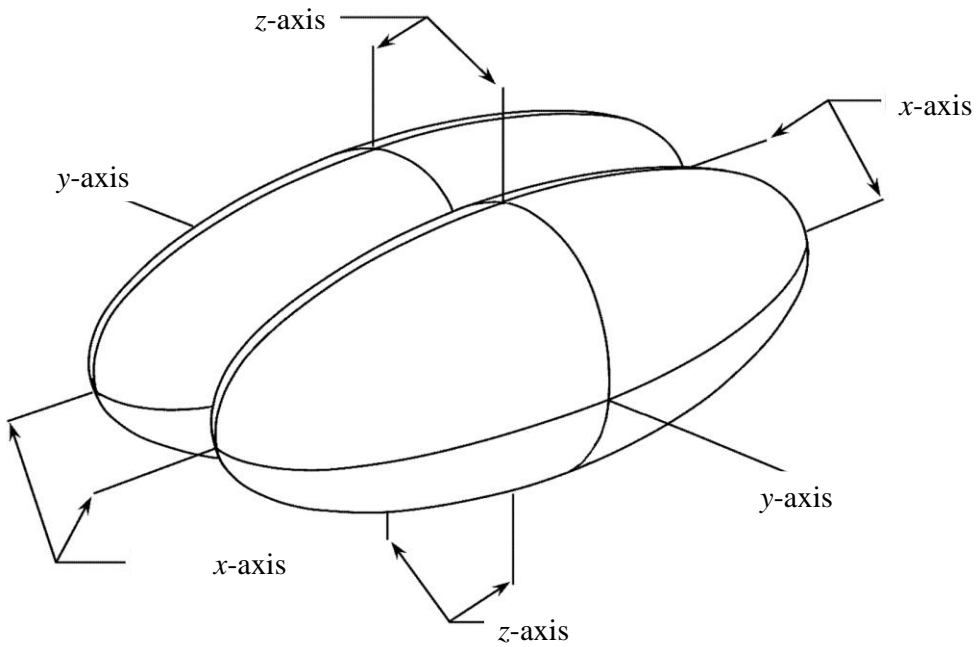
Figure 2.14. Eyellipse coordinate system (SAE J941, 2010)

5%

Tangent cutoff line

z-axis length/2

95%

46.7 mm

Side view angle (β)

$\beta = 18.6$ – cushion angle

103.2 mm

x-axis length/2

Eyellipse centroid
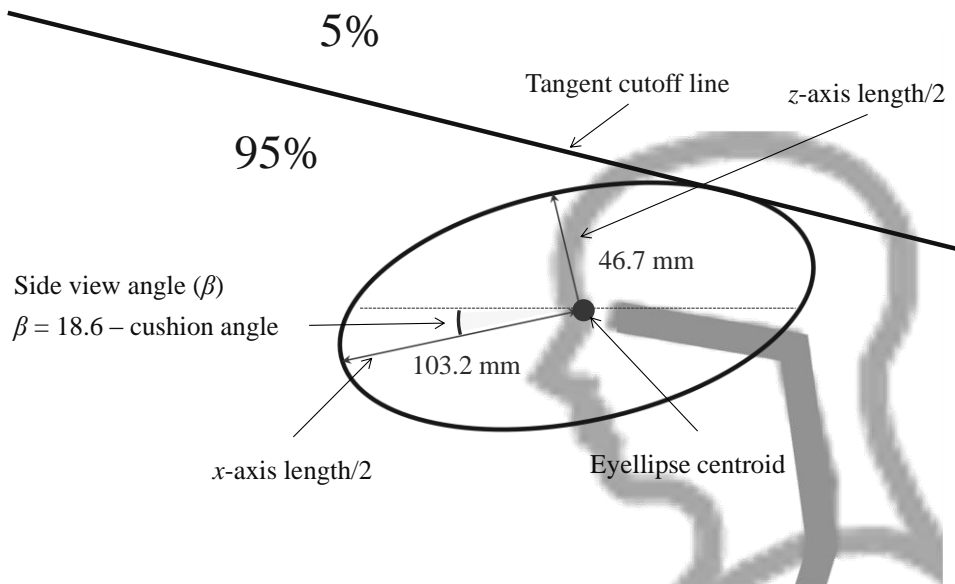
Figure 2.15. 95% SAE tangent cutoff eyellipse with longer than 133 mm seat travel

Table 2.2. Sizes of SAE tanget cutoff eyellipses (SAE J941, 2010)

Seat travel length (mm)	Tangent cutoff percentile	x-axis length (mm)	z-axis length (mm)
1 ~ 133	95%	173.8	93.4
	99%	241.1	132.1
> 133	95%	206.4	93.4
	99%	287.1	132.1

(a) IR measuring system	(b) Eye location measurement device

Figure 2.16. Measurement of an eye location by H-point machine

Figure 2.17. Measurement of a head contour using H-point machine (Reed et al., 2001)
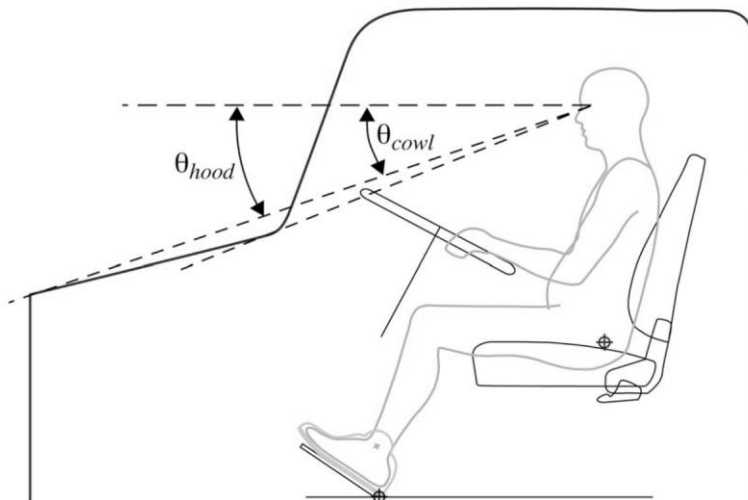
Figure 2.18. Design of windshield height based on MIL-STD-1472F

(Parkinson et al., 2007)

2.3. HL and EL prediction models

Prediction models have been developed to predict a driver's HL and EL. SAE J1517 (2011) proposed horizontal HL prediction models for 2.5^{th}, 5th, 10th, 50th, 90th, 95th, and 97.5^{th} %ile of US drivers (Equation 2.2) as shown in Figure 2.19. Horizontal HL prediction models of SAE J1517 used H30 and $H30^2$ as independent variables. According to the nonlinear characteristics of the SAE J1517's models, predicted HL distribution shows a curve as shown in Figure 2.18. Meanwhile, the SAE J1517's models were developed based on various stature ranges ($2.5^{th} \sim 97.5^{th}$ %ile) of US drivers.
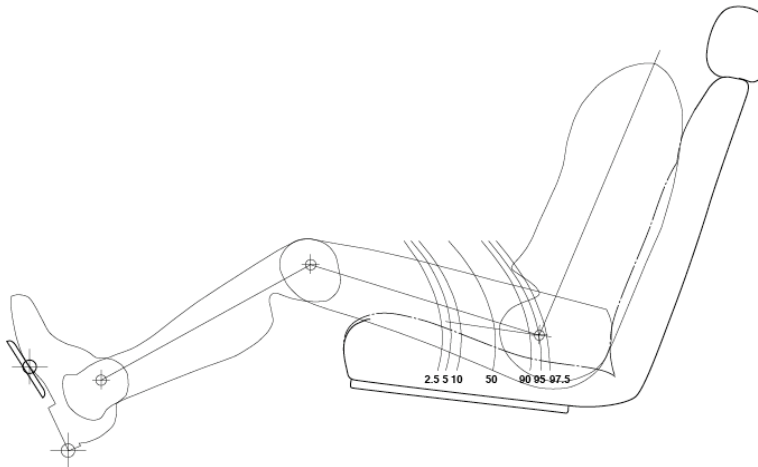
$$HLx_{2.5} = 687.1 + 0.895 \times H30 - 0.0021 \times H30^2$$
$$HLx_{5} = 692.6 + 0.981 \times H30 - 0.0023 \times H30^2$$
$$HLx_{10} = 715.9 + 0.969 \times H30 - 0.0023 \times H30^2$$
$$HLx_{50} = 793.7 + 0.903 \times H30 - 0.0022 \times H30^2$$
$$HLx_{90} = 885.0 + 0.735 \times H30 - 0.0020 \times H30^2$$
$$HLx_{95} = 913.7 + 0.672 \times H30 - 0.0020 \times H30^2$$
$$HLx_{97.5} = 936.6 + 0.614 \times H30 - 0.0019 \times H30^2$$

Equation 2.2

where: HLx_5 = horizontal location of hip for a 5th %ile US driver,
          H30 = seat height (z coordinate of the SgRP, measured vertically from AHP)

Figure 2.19. Prediction models of horizontal hip location using a seat height

(SAE J1517, 2011)

Horizontal and vertical EL prediction models of SAE J941 (2010) were developed based on OPL variables as shown in Figure 2.20. SAE J941 (2010) proposed EL prediction models to predict the centroid location (EL_x, EL_y, and EL_z) of an eyellipse and all the prediction models only considered OPL variables as independent variables. For example, the EL_x prediction model includes pedal reference point (PRP) x coordinate (L1), steering wheel center to PRP_x (L6), seat height (H30), transmission type (t). However, the SAE J941 didn't indicate the performance of the prediction models, so that a user doesn't know about prediction accuracy of the models.

Meanwhile, Reed et al. (2002) developed prediction models of HL and EL based on the statistical linear relationship among a driver's anthropometric variables, OPL variables, and seat configuration variables. The Reed et al. measured 68 US drivers' HL and EL using a digitizer in various package conditions (e.g., coupe, sedan, and SUV) and developed HL and EL prediction models based on participants' anthropometric dimensions (stature and sitting height/stature), OPL variables (e.g., steering wheel location), and seat configuration variable (cushion angle) by stepwise regression analysis (Table 2.3).
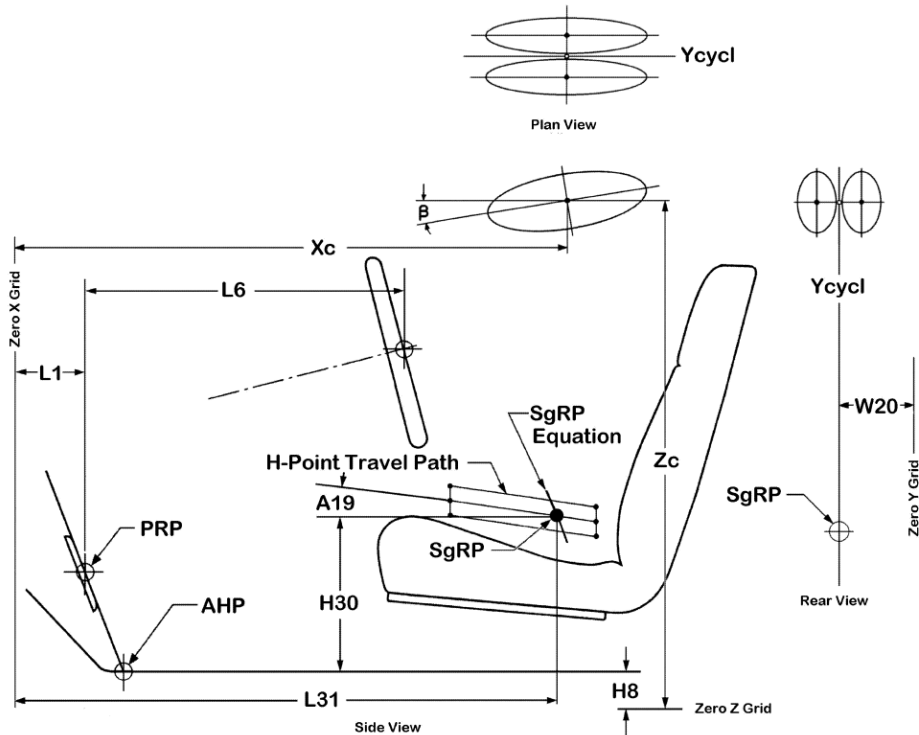
$$EL_x \quad = L1 + 664 + 0.587 \times L6 - 0.176 \times H30 - 12.5 \times t$$

$$EL_{y\text{-left}} \quad = W20 - 32.5$$

$$EL_{y\text{-right}} = W20 + 32.5$$

$$EL_z \quad = H8 + 638 + H30$$

Equation 2.3

Where: AHP = accelerator heel point,

EL = eye location,

H8 = AHP z coordinate,

H30 = seat height (z coordinate of the SgRP, measured vertically from AHP),

L1 = PRP x coordinate,

L6 = steering wheel center to PRP,

PRP = pedal reference point,

T = transmission type (1 with clutch pedal, 0 without clutch pedal),

W20 = SgRP y coordinate

Figure 2.20. Prediction models of eye location using OPL variables (SAE J941, 2010)

Table 2.3. Hip & eye location prediction models
using a driver's anthropometric and OPL variables (Reed et al., 2002)

Variable (mm or °)	Intercept	Stature (mm)	Sitting Height/ Stature	Seat Height (H30; mm)	SW to BOF$_x$ (L6; mm)	Cushion Angle (L27; °)	Adj. R^2	RMSE
Hip$_x$ reBOF	84.8	0.4659	-430.1	-0.1732	0.4479	-1.04	.78	35.9
Hip-to-eye angle	-72.7	0.0064	115.7	-	0.0147	0.11	.20	3.9
Eye$_x$ reBOF	-836.6	0.5842	916.6	-0.1559	0.6101	-	.71	50.9
Eye$_z$ reAHP	-267.1	0.3122	679.9	1.0319	0.0292	-	.89	21.8
Eye$_x$ reHip	-916.0	0.1187	1347.2	-	0.1563	1.15	.23	41.7
Eye$_z$ reHip	-261.5	0.3336	675.8	-	-0.0544	-	.72	22.9
Ankle$_x$ reBOF	-300.2	0.0400	467.6	0.1746	0.1358	1.3	.32	18.0
Ankle$_x$ reAPedal	46.1	-0.0466	-	-	-	-	.05	23.2
Ankle$_z$ reAHP	8.4	0.0312	-	0.1236	-	0.55	.25	13.1
Knee angle	69.1	-0.0071	61.3	-0.0321	0.0829	-0.59	.44	7.7
Head angle	-156.2	0.0092	137.5	-	-	-	.03	10.6
Neck angle	16.1	-0.0120	-	-	0.0109	-	.04	7.7
Thorax angle	-42.7	0.0050	45.2	-	0.0128	-	.03	6.1
Abdomen angle	-94.5	0.0109	184.5	-	0.0222	-	.09	9.7
Pelvis angle	-16.3	0.0102	90.2	-	0.0177	0.39	.04	10.0

Note: linear model created by multiplying each term in the table by the value of the column variable and adding a constant intercept. AHP = accelerator heel point; APedal = accelerator pedal; BOF = ball of foot; SW = steering wheel.

2.4. Geometric equations for a workstation design

Geometric equations of HL and EL were developed based on a user's anthropometric and posture variables to design an ergonomics workspace. You et al. (1997) developed design equation (Equation 2.4) to design a bus driver's workspace; for example, the horizontal distance from the bus accelerate pedal reference point (APRT) to neutral seat reference point (NSRP) can be determined by the geometric equation (Equation 2.4) of a driver's lower-body anthropometric data (e.g., femoral link length) and driving posture (e.g., knee flexion).

Jung et al. (2010) developed geometric equations of a pilot's EL and neutral seat reference point (NSRP) to design a helicopter cockpit layout based on pilots' anthropometric variables, posture variables, and cockpit configuration variables. For example, NSRP prediction model (Figure 2.22_a) consists of a pilot's anthropometric variables (popliteal height and buttock-popliteal length), posture variables (knee flexion angle and hip flexion angle), and footwear bottom height. Design eye point (DEP) prediction model (Figure 2.22_b) consists of a seat reference point, a pilot's posture variables (trunk extension angle and neck flexion angle) and anthropometric variables (acromial height and eye-to-neck length).
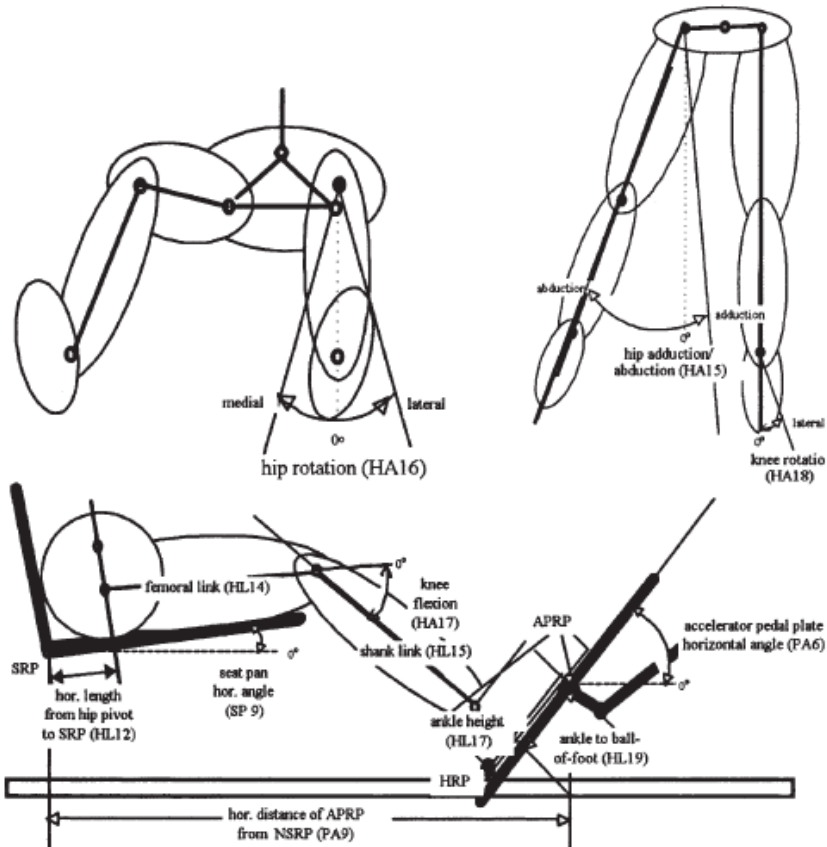
Horizontal distance of APRP from NSRP

$= \{(HL12 + HL14) \times \cos(SP9) + (HL15 + HL17) \times \sin(90° + SP9 - HA17)$

$+ HL19 \times \cos(PA6)\} \times \cos(HA15 + HA16 + HA18)$

Equation 2.4

where: APRP = accelerator pedal reference point, NSRP = neutral seat reference point,

HL12 = horizontal length from hip pivot to SRP, HL14 = femoral link; HL15 = shank link,

HL17 = ankle pivot height from floor with shoes, HL19 = horizontal length from ankle pivot to ball-of-foot,

HA15 = hip abduction; HA16 = hip rotation, HA17 = knee flexion, HA18 = knee rotation,

SP9 = horizontal angle of seatpan, PA6 = horizontal angle of accelerator pedal plate

Figure 2.21. Prediction models of hip location using the geometric relationship

(You et al., 1997)
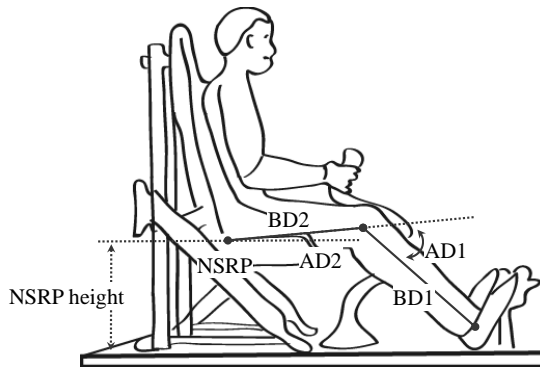
$$\text{NSRP height} = BD1 \times \sin(\theta_1) - BD2 \times \sin(\theta_2) + 2.5 \qquad \text{Equation 2.5}$$

Where: BD1 = popliteal height,
        BD2 = buttock-popliteal length,
        NSRP = neutral seat reference point,
        θ_1 = knee flexion angle,
        θ_2 = hip flexion angle

(a) Neutral seating reference point prediction model
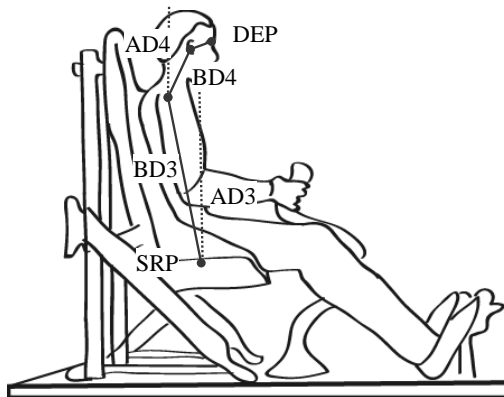
$$\text{DEP height} = \text{SRP height} + BD3 \times \cos(\theta_3) + BD4 \times \cos(\theta_4) \qquad \text{Equation 2.6}$$

where: BD3 = acromial height,
        BD4 = eye-to-neck length,
        SRP = seat reference point,
        θ_3 = trunk extension angle,
        θ_4 = neck flexion angle

(b) Design eye location prediction model

Figure 2.22. Prediction models using the geometric relationship (Jung et al., 2010)

Lastly, ANSI/HFES 100 (2007) proposed geometric equation (Equation 2.7) of seatpan height to design a computer workstation based on the geometric relationship between a user's anthropometric variables and seat configuration variables. The ANSI/HFES 100's model consists of popliteal height, buttock-popliteal length, seatpan angle, seat pan depth (SPD) and heel height as shown in Figure 2.23.
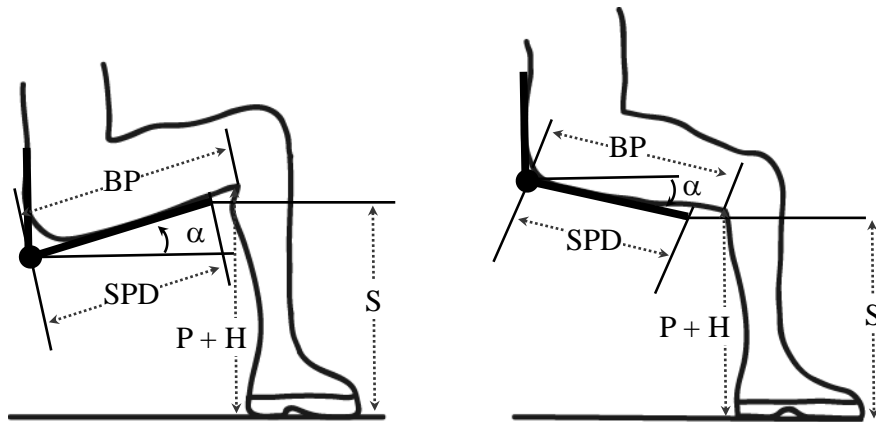
$$S = P + H - (BP - SPD) \times \sin(\theta)$$ Equation 2.7

where: BP = buttock-popliteal length,
          H = heel height,
          S = seat height,
          SPD = seat pan depth,
          P = popliteal height,
          θ = seat pan angle

Figure 2.23. Design equation of seat height using the geometric relationship

(ANSI/HFES 100, 2007)

2.5. Sitting strategies

Several researches have been conducted to design/evaluate an ergonomics driver seat by user preferred posture/seating pressure distribution. Park (2006) classified 128 Korean male drivers' postures into 5 representative postures by cluster analysis using the joint angles of participants. Andreoni et al. (2002) classified 3 sitting strategies for upper-body (lumbar, dorsal, and dorsal scapular strategy) and 3 strategies for lower-body (ischiatic, intermediate, and trochanteric strategy) based on the visual observation of 8 male drivers' seating pressure distributions of seatback and seatpan (Figure 2.24).

Although several researches of the sitting strategy have been conducted to design an ergonomics driver seat, the Andreoni et al.'s sitting strategy classification method is based on an analyst's visual judgment, without objective information. Moreover, to apply the classified sitting strategies into the design stage of a driver seat, factors (e.g., driver's gender, OPL condition) which can affect to the sitting strategy need to be identified clearly; nevertheless, Park (2006) did not analyze the characteristics of classified sitting strategies.
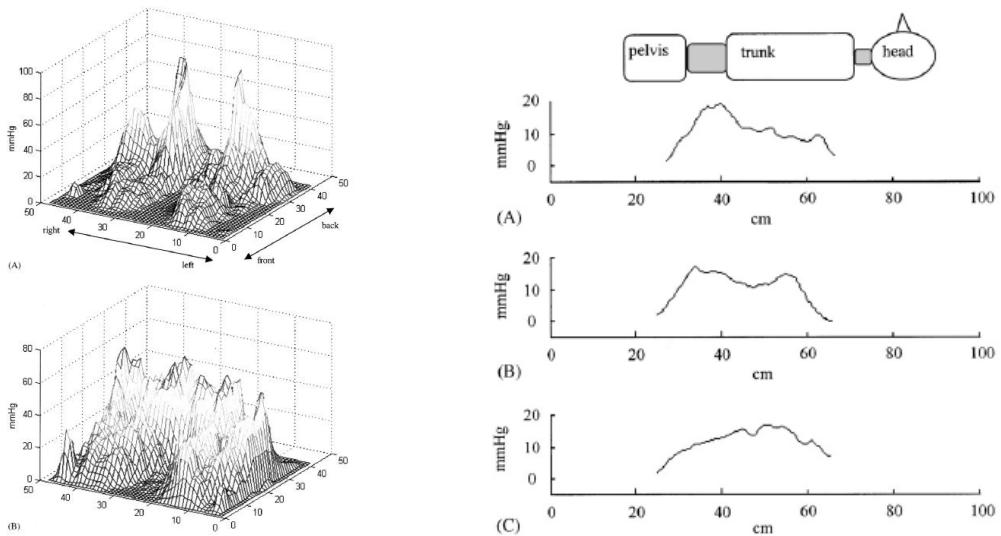
(a) Lower-body seating pressure   (b) Upper-body seating pressure

Figure 2.24. Classified sitting strategies based on

the visual observation of seating pressures (Andreoni et al., 2002)

Meanwhile, to supplement the previous research's ambiguous analysis of the sitting strategy, Choi (2012) analyzed Korean drivers' preferred seating pressures and classified sitting strategies using body pressure ratio (BPR) in a quantitative manner. The BPR was proposed by Mergl et al. (2005) and Zenk et al. (2006), it is seating pressure ratio (%) of a driver's each 17 body parts (9 parts for upper-body and 8 parts for lower-body). The body parts were defined by the driver's anthropometric body grids which were generated by the participant's back length, hip width, and buttock-popliteal lengths. The body grids were used to define the region of upper-body and lower- body part. Choi (2012) generated each participant's body grid using their anthropometric data and analyzed their BPR from the total pressure of upper-/lower-body. Choi analyzed 20 males and 20 females of Korean driver's BPR and classified Korean drivers' sitting strategies by cluster analysis into 3 upper-body (mid-back & scapular, mid-back & lumbar, and lumbar sitting strategy; Figure 2.25_a) and 3 lower-body (hip concentrated, hip & mid-thigh concentrated, and hip & mid-thigh distributed sitting strategy; Figure 2.25_b).

Choi (2012)

Mid-back & Scapular — 15.8 | 17.4 | 26.9 | 22.5 — **37%**

Mid-back & Lumbar — 11.3 | 11.0 | 25.8 | 27.8 — **43%**

Lumbar — 4.6 | 4.0 | 31.0 | 33.4 — **20%**

Matching

Andreoni et al. (2002)

Dorsal scapular — **38%**

Dorsal — **50%**

Lumbar — **12%**

(a) Upper-body sitting strategies

Choi (2012)

Hip Concentrated — 22.1 | 26.6 | 13.1 | 15.4 — **41%**

Hip & Mid-thigh Concentrated — 17.8 | 21.7 | 15.7 | 17.0 — **45%**

Hip & Mid-thigh Distributed — 12.7 | 20.2 | 19.4 | 19.4 — **14%**

Matching

Andreoni et al. (2002)

Ischiatic — **63%**

Intermediate — **12%**

Trochanteric — **25%**

(b) Lower-body sitting strategies

Figure 2.25. Classified sitting strategies based on
the quantitative analysis of seating pressures (Choi, 2012)

Chapter 3   DEVELOPMENT OF HIP & EYE LOCATION PREDICTION MODELS

3.1. Measurement of driving postures using a motion capture system

3.1.1. Participants

Forty participants (male: 20; female: 20) in 20s ~ 50s having at least two years of driving experience participated in driving posture measurement. To recruit participants variously in stature, 3 categories ($<$ 33%, 33% ~ 67%, and $>$ 67%) were formed using corresponding anthropometric data of Korean males and females (Size Korea, 2010). The average height of the male participants was 173 cm (SD = 6.2; range = 157 cm ~ 181 cm) and female was 161 cm (SD = 5.8; range = 150 cm ~ 170 cm; Appendix A).

3.1.2. Apparatus

The present study used a reconfigurable seating buck and a motion capture system to measure driving postures of the participants (Figure 3.2). The seating buck was fabricated to synchronized with virtual driving scenery projected on the front screen (width = 180 cm, height = 160 cm) and it designed to reconfigurable for 3 different occupant package layout conditions (H30 height; coupe = 176 mm; sedan = 240 mm; SUV = 305 mm). The fabricated seat (Equus, Hyunday-Kia Motors, Korea) on a seating buck has motorized controller that a participant can change the seat position, seatpan length, seatpan angle, seatback angle, and headrest height in which they preferred. Totally, 6 Hawk-I digital cameras (Motion Analysis Co., USA) were used to record driving posture of the participants (Figure 3.3).
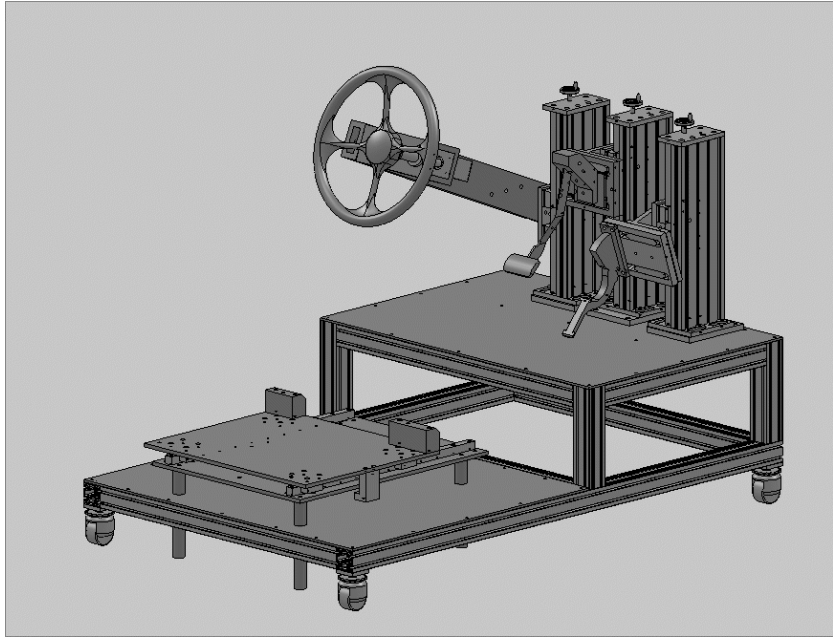
Figure 3.1. Reconfigurable seating buck for 3 OPL conditions (coupe, sedan, SUV)

Figure 3.2. Motion capture system to measure a participant's driving posture

3.1.3. Experimental procedure

The posture measurement in the seating buck was conducted in three steps (Figure 3.3). First, the research purpose and experimental process were introduced to the participant and then a written informed consent was obtained. The 21 body sizes (Figure 3.4) of the participant were obtained followed by RAMSIS anthropometry protocol (Speyer, 2005) using a Martin's anthropometer (TTM, Tsutsumi Co., Japan). The measurements were made twice for each anthropometric dimension (Figure 3.5) and then their average value was used. If the difference of two measurements was greater than 5 mm, additional measurements were taken. Next, 26 reflective markers (Ø = 1.2 cm) were attached on the body of participant (Figure 3.6). Second, the participant was asked to find their preferred seating position of the seat while self-adjustment driving for 10 minutes. After the participant found his/her preferred seat position, the participants were asked to hold 3-to-9 steering wheel position with both hands and the driving posture was captured by a motion capture cameras (Figure 3.7). Lastly, a debriefing was conducted and the participant was compensated.
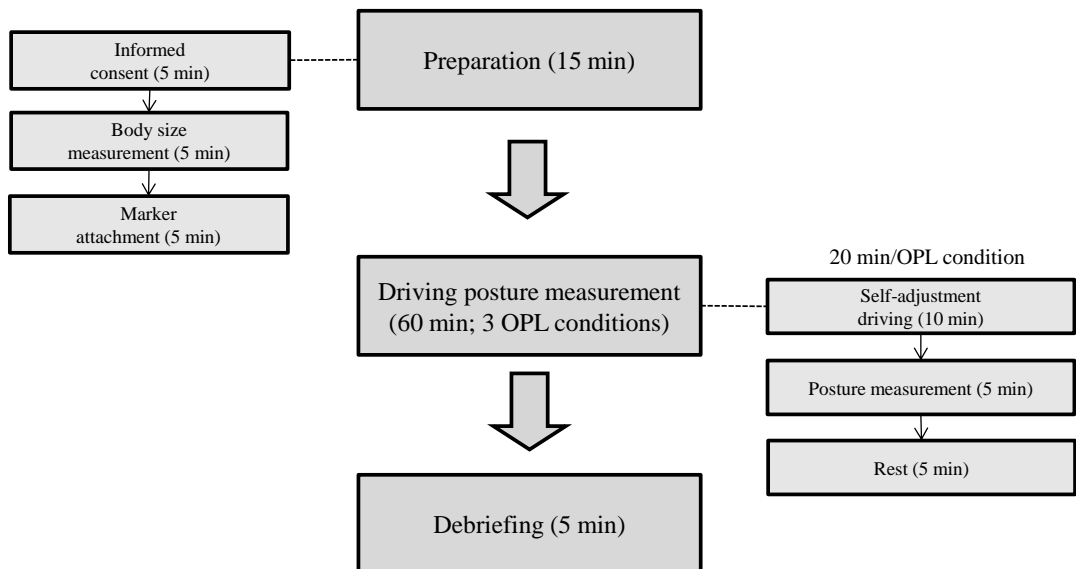
Figure 3.3. Experimental procedure using a motion capture system
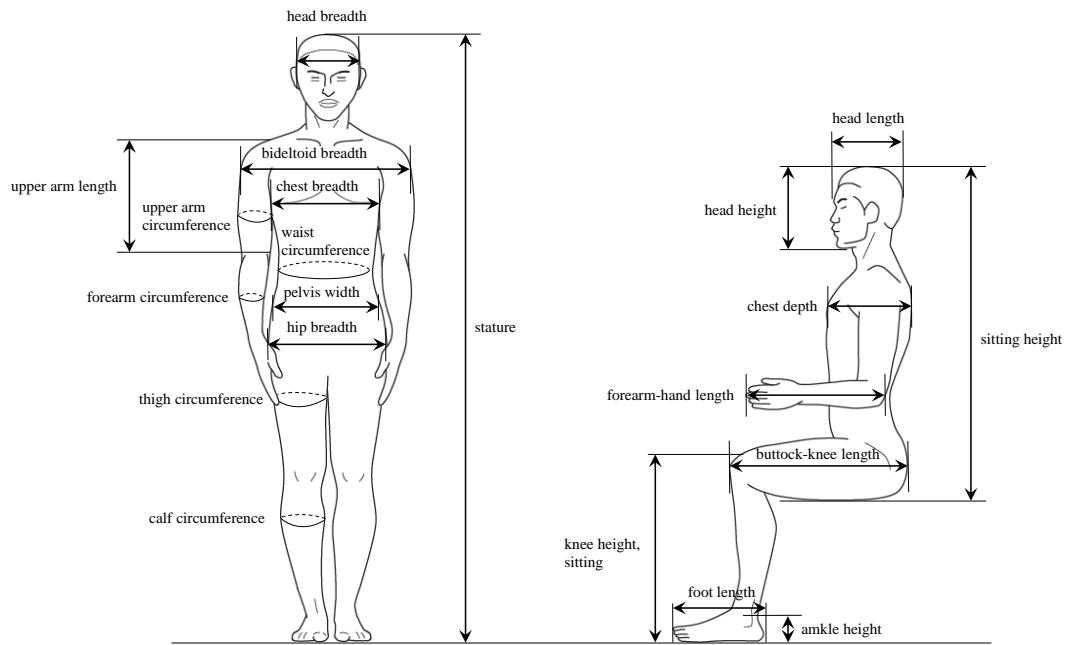
Figure 3.4. Anthropometric measurements

Figure 3.5. Measurement of a participant's body sizes

Figure 3.6. Reflective markers on the whole-body

Figure 3.7. Measurement of a participant's preferred driving posture

3.2. Reconstruction of a driving posture using RAMSIS

To construct a database (DB) of the HLs, ELs, and driving postures (joint angles) of the participants, captured driving postures were reconstructed using RAMSIS® (Human Solution GmbH, Germany) through three stages: generation of a humanoid and reference points, modification of reference point positions, and synchronization of reference point positions to reflective marker positions. In the first stage, a humanoid for a driver was generated using the 21 anthropometric measurements of the driver. Next, 26 reference points were generated on the skin surface of the humanoid by referring to the locations of the 26 reflective markers attached to the driver (Figure 3.8$_a$). In the second stage, the locations of the reference points were modified by referring to the distances between the reflective markers obtained from the captured marker data in standing (Figure 3.8$_b$). In the third stage, the positions of the reference points were synchronized with those of the reflective markers captured in driving by the posture reconstruct function (*Animation Simulator*) of RAMSIS (Figure 3.8$_c$). Lastly, the HL, EL, and the joint angles of the head, neck, torso, hip, knee, and ankle of the driver were extracted by RAMSIS (Figure 3.9). There 3 steps were repeated to extract the 40 participants' HLs, ELs, and joint angles.
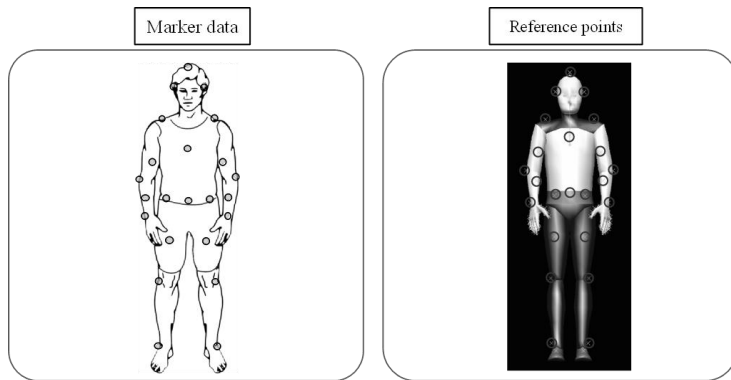
(a) Generation of reference points

Modification of reference point locations using distance information of the markers
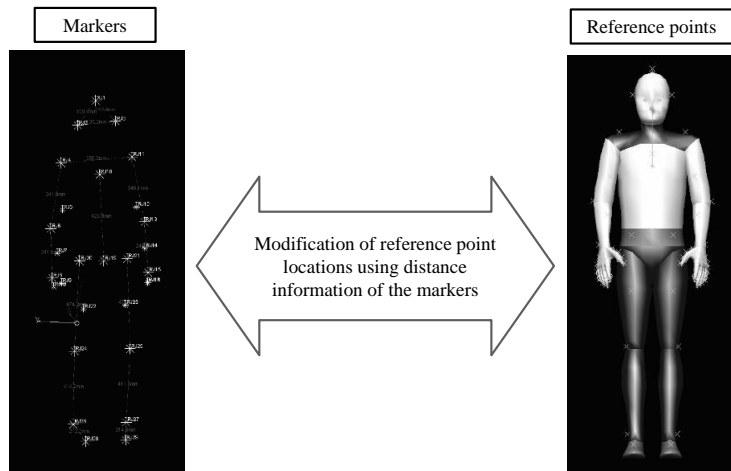
(b) Modification of reference point locations
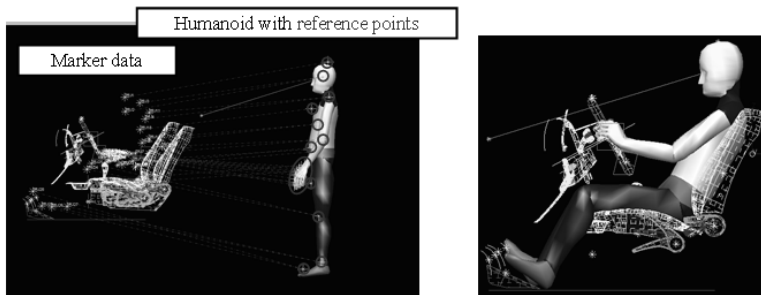
(c) Reconstruction of a driver's posture

and extraction of hip & eye locations, and joint angles

Figure 3.8. Reconstruction process of the measured posture using a RAMSIS humanoid
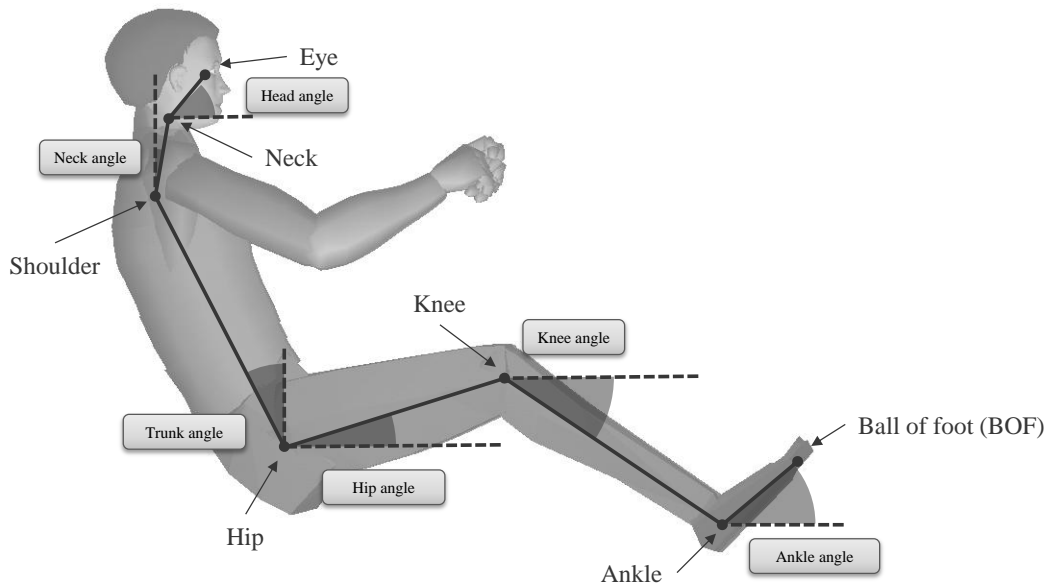
Figure 3.9. Six joint angles to analyze a driving posture

3.3. Development of statistical geometric models for HL and EL

Statistical geometric models (SGMs) of HL and EL were developed by incorporating the geometric relationships between HL, EL, anthropometric dimensions, and driving postures and the statistical relationships between body link lengths and surface landmark lengths. As displayed in Figure 3.10, the SGM for horizontal HL (Hip_x reBOF) was constructed using the link lengths (femoral, shank, and foot links) and related joint angles (hip, knee, and ankle angles) of the leg and foot; then, regression coefficients for Hip_x reBOF were constructed by multiple regression analysis based on the geometric equations to consider the conversion relationships between the link lengths and the corresponding surface landmark lengths (buttock-popliteal length, knee height, and foot length). The same procedure was applied to the development of SGMs for EL. As illustrated in Figure 3.11, the geometric equation for horizontal EL (Eye_x reBOF) was constructed using the link lengths (trunk, cervical link, and head link) and joint angles (trunk, neck, and head angles) of the trunk and head in addition to those of the leg and foot; then, regression coefficient for Eye_x reBOF and Eye_z reAHP were constructed by multiple regression

43

analysis to consider the conversion relationships between the trunk and head link lengths and the corresponding surface landmark lengths (sitting height and head length) in addition to those of the leg and foot.

$$\text{Hip}_x \, re\text{BOF} = \{FL_1 \times \cos(\theta_{ankle})\} + \{SL \times \cos(\theta_{knee})\} + \{FL_2 \times \cos(\theta_{hip})\}$$

where: BOF = ball of foot,
  FL_1 = foot link length,
  FL_2 = femoral link length,
  SL = shank length,
  θ_{hip} = hip angle,
  θ_{knee} = knee angle,
  θ_{ankle} = ankle angle
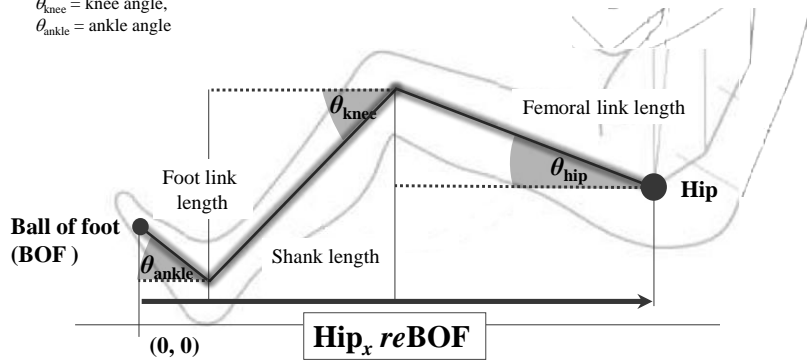
Figure 3.10. Geometric equation for horizontal HL

$\text{Eye}_x \, re\text{BOF}$

$= \{FL \times \cos(\theta_{ankle})\} + \{LL \times \cos(\theta_{knee})\} + \{UL \times \cos(\theta_{hip})\}$
$+ \{TL \times \sin(\theta_{trunk})\} - \{NL \times \text{sie}(\theta_{neck})\} - \{HL \times \cos(\theta_{head})\}$

where: BOF = ball of foot,
  FL = foot link length,
  LL = lower-leg link length,
  UL = upper-leg link length,
  TL = trunk link length,
  NL = neck link length,
  HL = head link length,
  θ_{hip} = hip angle,
  θ_{knee} = knee angle,
  θ_{ankle} = ankle angle,
  θ_{trunk} = trunk angle,
  θ_{neck} = neck angle,
  θ_{head} = head angle,
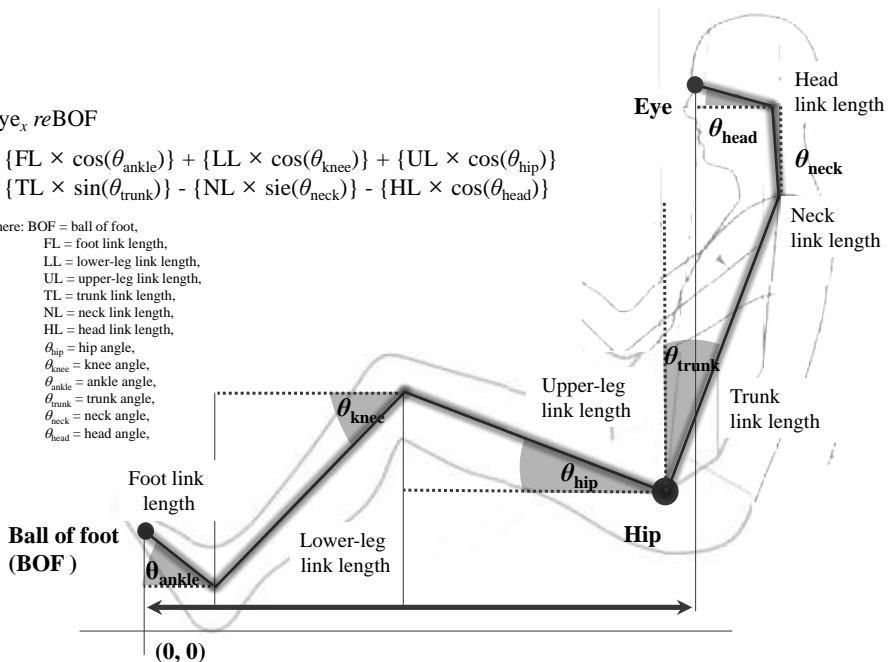
Figure 3.11. Geometric equation for horizontal EL

The SGM of HL was represented by the statistical geometric equations (Equation 4.1, 4.2) which include a driver's lower-body surface landmark measurement dimensions (foot length, knee height, and buttock popliteal length) and related joint angles (ankle, knee, and hip angles), and link length conversion ratios (regression coefficients) as shown in Figure 3.11; the SGM of EL (Equation 4.3, 4.4) includes lower- and upper-body surface landmark measurement dimensions (foot length, knee height, buttock popliteal length, sitting height, and head length), related joint angles (ankle, knee, hip, trunk, neck, and head angles) and link length conversion ratios as shown in Figure 3.12. Moreover, the SGMs of Eye_x reHip and Eye_z reHip were developed to predict a driver's eye location from a driver's hip location. The developed Hip_x reBOF and Hip_z reAHP models' adjusted coefficient of determination (adj. R^2) are 0.84 and 0.86 and root mean squared errors ($RMSE$) are 21.1 mm and 25.2 mm each. Next, the developed Eye_x reBOF and Eye_z reAHP models' adj. R^2 are 0.85 and 0.82; $RMSE$ are 29.2 mm and 29.9 mm. Next, the developed Eye_x reHip and Eye_z reHip models' adj. R^2 are 0.85 and 0.69; $RMSE$ are 22.6 mm and 26.9 mm. Lastly, these models (Hip_x reBOF, Hip_z reAHP, Eye_x reBOF, Eye_z reAHP, Eye_x reHip, and Eye_z reHip) were compared with the Reed et al. (2002)'s models in terms of prediction accuracy (adj. R^2 and $RMSE$).

$$\text{Hip}_x\,re\text{BOF} = 148 + \{0.684 \times \text{BPL} \times \cos(\theta_{\text{hip}})\} + \{0.618 \times \text{KH} \times \cos(\theta_{\text{knee}})\}$$
$$+ \{0.248 \times \text{FL} \times \cos(\theta_{\text{ankle}})\}$$

Equation 4.1

Adj. $R^2 = 0.84$; $RMSE = 21.1$

$$\text{Hip}_z\,re\text{AHP} = 128 - \{0.660 \times \text{BPL} \times \sin(\theta_{\text{hip}})\} + \{0.648 \times \text{KH} \times \sin(\theta_{\text{knee}})\}$$
$$- \{0.265 \times \text{FL} \times \sin(\theta_{\text{ankle}})\}$$

Equation 4.2

Adj. $R^2 = 0.86$; $RMSE = 25.2$

Where: BOF = ball of foot,
   AHP = accelerator heel point,
   BPL = buttock popliteal length,
   KH = knee height,
   FL = foot length,
   θ_{hip} = hip angle,
   θ_{knee} = knee angle,
   θ_{ankle} = ankle angle

(0, 0)
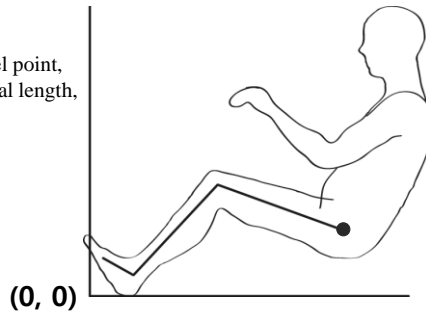
Figure 3.12. The statistical geometric models for Hip$_x$ reBOF and Hip$_z$ reAHP

$$\text{Eye}_x\,re\text{BOF} = 132 + \{0.513 \times \text{BPL} \times \cos(\theta_{\text{hip}})\} + \{0.695 \times \text{KH} \times \cos(\theta_{\text{knee}})\}$$
$$+ \{0.314 \times \text{FL} \times \cos(\theta_{\text{ankle}})\} + \{0.486 \times \text{SH} \times \sin(\theta_{\text{trunk}})\} - \{0.901 \times \text{HL} \times \sin(\theta_{\text{neck}})\}$$
$$- \{0.100 \times \text{HL} \times \cos(\theta_{\text{head}})\}$$

Equation 4.3

Adj. $R^2 = 0.85$; $RMSE = 29.2$

$$\text{Eye}_z\,re\text{AHP} = 172 - \{0.409 \times \text{BPL} \times \sin(\theta_{\text{hip}})\} + \{0.696 \times \text{KH} \times \sin(\theta_{\text{knee}})\}$$
$$- \{0.369 \times \text{FL} \times \sin(\theta_{\text{ankle}})\} + \{0.671 \times \text{SH} \times \cos(\theta_{\text{trunk}})\} + \{0.150 \times \text{HL} \times \cos(\theta_{\text{neck}})\}$$
$$- \{0.324 \times \text{HL} \times \sin(\theta_{\text{head}})\}$$

Equation 4.4

Adj. $R^2 = 0.82$; $RMSE = 29.9$

Where: BOF = ball of foot,
   AHP = accelerator heel point,
   BPL = buttock popliteal length,
   SH = sitting height,
   HL = head length,
   KH = knee height,
   FL = foot length,
   θ_{hip} = hip angle,
   θ_{knee} = knee angle,
   θ_{ankle} = ankle angle,
   θ_{trunk} = trunk angle,
   θ_{neck} = neck angle,
   θ_{head} = head angle

(0, 0)
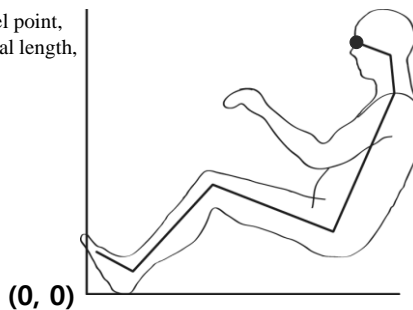
Figure 3.13. The statistical geometric models for Eye$_x$ reBOF and Eye$_z$ reAHP

$$\text{Eye}_x \, re\text{Hip} = -86.3 + \{0.525 \times \text{SH} \times \sin(\theta_{\text{trunk}})\} - \{0.907 \times \text{HL} \times \sin(\theta_{\text{neck}})\} \qquad \text{Equation 4.5}$$
$$- \{0.081 \times \text{HL} \times \cos(\theta_{\text{head}})\}$$
$$\text{Adj. } R^2 = 0.85; \, RMSE = 22.6$$

$$\text{Eye}_z \, re\text{Hip} = -62.6 + \{0.682 \times \text{SH} \times \cos(\theta_{\text{trunk}})\} + \{0.729 \times \text{HL} \times \cos(\theta_{\text{neck}})\} \qquad \text{Equation 4.6}$$
$$- \{0.242 \times \text{HL} \times \sin(\theta_{\text{head}})\}$$
$$\text{Adj. } R^2 = 0.69; \, RMSE = 26.7$$

Where: SH = sitting height,
HL = head length,
θ_{trunk} = trunk angle,
θ_{neck} = neck angle,
θ_{head} = head angle

(0, 0)
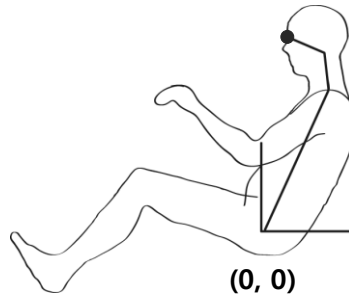
Figure 3.14. The statistical geometric models for $\text{Eye}_x \, re\text{Hip}$ and $\text{Eye}_z \, re\text{Hip}$

Meanwhile, the present study developed simple statistical geometric models (simple SGMs) to increase a usability of the SGMs using a driver's stature. Figure 3.14 shows the developed simple SGMs of $\text{Hip}_x \, re\text{BOF}$ and $\text{Hip}_z \, re\text{AHP}$ by changing the independent variables (buttock-popliteal length, knee height, and foot length) to stature. Adj. R^2 of the simple SGMs are 0.83 for $\text{Hip}_x \, re\text{BOF}$ and 0.85 for $\text{Hip}_z \, re\text{AHP}$. Next, $RMSE$ are 21.6 mm for $\text{Hip}_x \, re\text{BOF}$ and 26.1 mm for $\text{Hip}_z \, re\text{AHP}$. This result shows that the simple SGMs have 0.01 smaller adj. R^2 than the complex ones for $\text{Hip}_x \, re\text{BOF}$ and $\text{Hip}_z \, re\text{AHP}$. Next, the simple SGMs have 0.5 mm and 0.9 mm larger $RMSE$ than the complex ones for $\text{Hip}_x \, re\text{BOF}$ and $\text{Hip}_z \, re\text{AHP}$. On the other hand $\text{Eye}_x \, re\text{BOF}$ and $\text{Eye}_z \, re\text{Hip}$ of simple SGMs shows 0.02 and 0.04 higher adj. R^2 than the complex ones. These results indicate that both the complex and simple models have similar prediction performances, so that an analyst can select the appropriate models by considering the anthropometric data.

$\text{Hip}_x \, re\text{BOF} = -17.2 + \{0.300 \times S \times \cos(\theta_{hip})\} + \{0.206 \times S \times \cos(\theta_{knee})\}$

Equation 4.7

$+ \{0.050 \times S \times \cos(\theta_{ankle})\}$

Adj. $R^2 = 0.83$; $RMSE = 21.6$

$\text{Hip}_z \, re\text{AHP} = 109 - \{0.221 \times S \times \sin(\theta_{hip})\} + \{0.207 \times S \times \sin(\theta_{knee})\}$

Equation 4.8

$- \{0.031 \times S \times \sin(\theta_{ankle})\}$

Adj. $R^2 = 0.85$; $RMSE = 26.1$

Where: BOF = ball of foot,
      AHP = accelerator heel point,
      S = stature,
      θ_{hip} = hip angle,
      θ_{knee} = knee angle,
      θ_{ankle} = ankle angle

(0, 0)
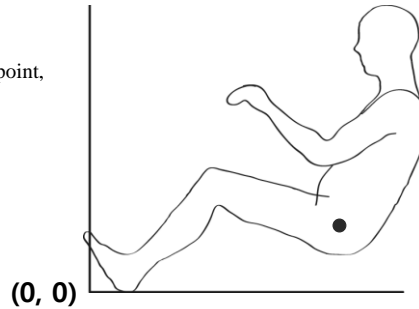
Figure 3.15. The simple statistical geometric models for $\text{Hip}_x \, re\text{BOF}$ and $\text{Hip}_z \, re\text{AHP}$

$\text{Eye}_x \, re\text{BOF} = -2.1 + \{0.199 \times S \times \cos(\theta_{hip})\} + \{0.226 \times S \times \cos(\theta_{knee})\}$

Equation 4.9

$+ \{0.064 \times S \times \cos(\theta_{ankle})\} + \{0.199 \times S \times \sin(\theta_{trunk})\} - \{0.136 \times S$

$\times \sin(\theta_{neck})\} + \{0.017 \times S \times \cos(\theta_{head})\}$

Adj. $R^2 = 0.87$; $RMSE = 27.2$

Equation 4.10

$\text{Eye}_z \, re\text{AHP} = 169 - \{0.147 \times S \times \sin(\theta_{hip})\} + \{0.200 \times S \times \sin(\theta_{knee})\}$

$- \{0.057 \times S \times \sin(\theta_{ankle})\} + \{0.258 \times S \times \cos(\theta_{trunk})\} + \{0.122 \times$

$S \times \cos(\theta_{neck})\} - \{0.048 \times S \times \sin(\theta_{head})\}$

Adj. $R^2 = 0.80$; $RMSE = 31.2$

Where: BOF = ball of foot,
      AHP = accelerator heel point,
      S = stature,
      θ_{hip} = hip angle,
      θ_{knee} = knee angle,
      θ_{ankle} = ankle angle,
      θ_{trunk} = trunk angle,
      θ_{neck} = neck angle,
      θ_{head} = head angle

(0, 0)
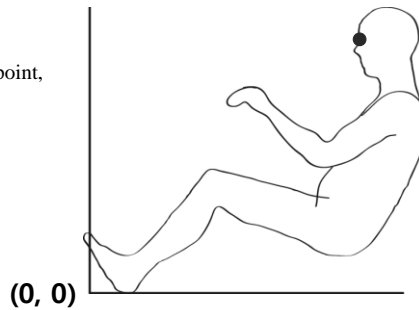
Figure 3.16. The simple statistical geometric models for $\text{Eye}_x \, re\text{BOF}$ and $\text{Eye}_z \, re\text{AHP}$

$$\text{Eye}_x \, re\text{Hip} = -67.7 + \{0.300 \times S \times \sin(\theta_{\text{trunk}})\} - \{0.114 \times S \times \sin(\theta_{\text{neck}})\}$$

Equation 4.11

$$-\{0.037 \times S \times \cos(\theta_{\text{head}})\}$$

Adj. $R^2 = 0.85$; $RMSE = 22.8$

$$\text{Eye}_z \, re\text{Hip} = -111 + \{0.236 \times S \times \cos(\theta_{\text{trunk}})\} + \{0.241 \times S \times \cos(\theta_{\text{neck}})\}$$

Equation 4.12

$$-\{0.029 \times S \times \sin(\theta_{\text{head}})\}$$

Adj. $R^2 = 0.73$; $RMSE = 25.1$

Where: S = stature,
θ_{trunk} = trunk angle,
θ_{neck} = neck angle,
θ_{head} = head angle

(0, 0)
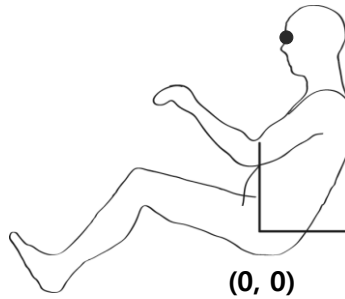
Figure 3.17. The simple statistical geometric models for Eye*x* *re*Hip and Eye*z* *re*Hip

Chapter 4 COMPARISON OF THE STATISTICAL GEOMETRIC MODELS AND REED ET AL.'S MODELS

4.1. Comparison of prediction performance

The prediction performances of SGMs have been evaluated in comparison with Reed et al.'s models in aspects of adj. R^2 and *RMSE*. While the adj. R^2 range of Reed et al. prediction models about hip and eye location is 0.23 ~ 0.89, the adj. R^2 range of SGMs is 0.69 ~ 0.86 (Table 4.1). Therefore, the SGMs have 1.6 times better prediction accuracy than Reed et al.'s models. Moreover, the *RMSE* of Reed et al.'s prediction models is 22.9 ~ 50.9 mm, the *RMSE* of SGMs is 21.1 ~ 29.9 mm. Therefore, the SGMs have 1.4 times smaller prediction error than Reed et al.'s models. Figure 4.1 shows the result of predicted HL and EL distributions (by SGMs and Reed et al.'s models) and measured ones. As a result, the predicted horizontal ELs by Reed et al.'s model (Eye$_x$ *re*BOF) seems to have large difference from measured ones; however, the predicted ELs by SGMs seems to have small difference from measured ones.

Table 4.1. Prediction performance evaluation: Reed et al.'s vs. statistical geometric models

Dependent variable	adj. R^2			*RMSE* (unit: mm)		
	Reed et al.'s model	simple SGMs	complex SGMs	Reed et al.'s model	simple SGMs	complex SGMs
Hip$_x$ *re*BOF	0.78	0.83	0.84	35.9	21.6	21.1
Eye$_x$ *re*BOF	0.71	0.87	0.85	50.9	27.2	29.2
Eye$_z$ *re*AHP	0.89	0.80	0.82	21.8	31.2	29.9
Eye$_x$ *re*Hip	0.23	0.85	0.85	41.7	22.8	22.6
Eye$_z$ *re*Hip	0.72	0.73	0.69	22.9	25.1	26.7

Note: *RMSE* = root mean squared error.
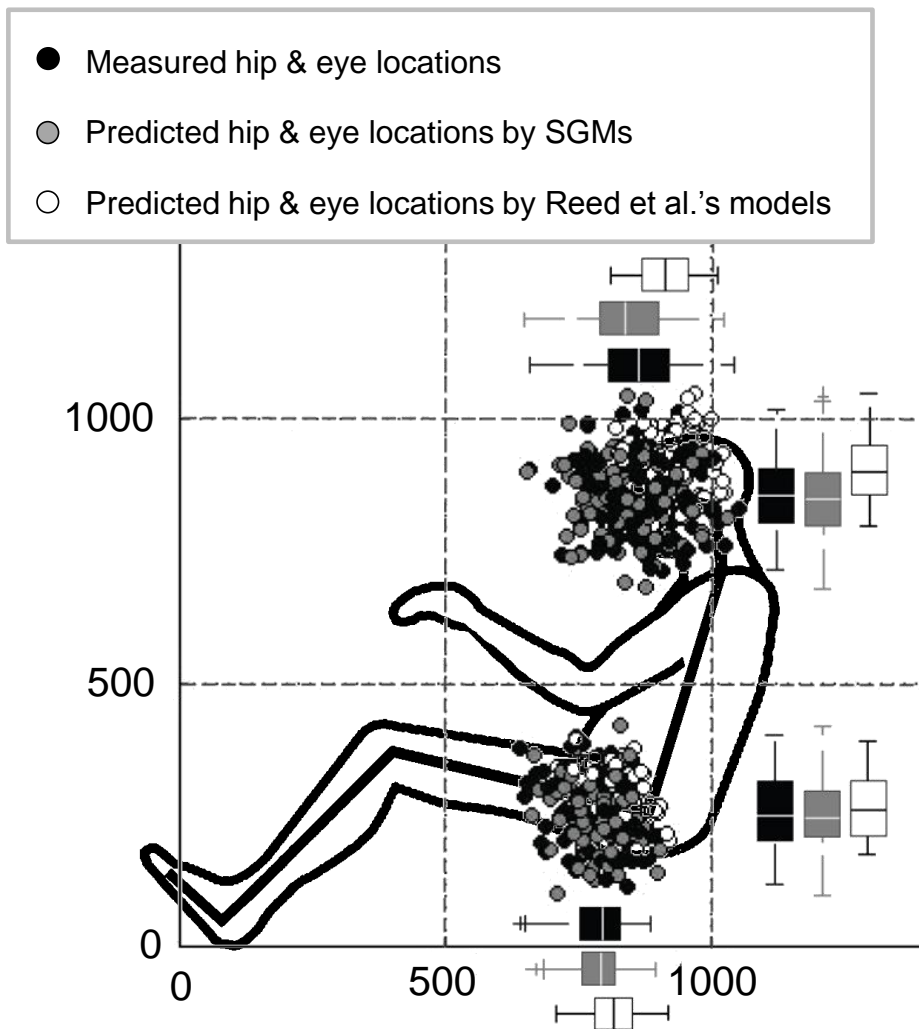
Figure 4.1. Predicted hip & eye locations by Reed et al.'s and SGMs, and measured ones

4.2. Comparison of prediction performance by occupant package layout types

The prediction performances of SGMs for different OPL types (coupe, sedan, and SUV) are also evaluated compared with the ones of Reed et al.'s models. The *RMSE* of Reed et al.'s models for different OPL types is 36.3 mm ~ 124.9 mm and the one of the SGMs is 17.6 mm ~ 35.8 mm. The *RMSE* of SGMs is 1.7 ~ 4.3 times lower than one of the

Reed et al.'s prediction models (Table 4.2). Therefore, the SGMs have more prediction stability than the Reed et al.'s models for different OPL conditions. In fact, the Reed et al.'s models used seat configuration (cushion angle) and OPL condition (seat height) as independence variables, so that the Reed et al.'s models are more sensitive from OPL conditions than the SGMs; however, the SGMs used a driver's anthropometric dimensions and joint angles as independence variables, not OPL conditions, so that the performances of SGMs for different OPL conditions are stable.

Table 4.2. Prediction performance evaluation by OPL types: Reed et al.'s models vs. SGMs

Dependent variable	OPL type	$RMSE$ (unit: mm)	
		Reed et al.'s models	Statistical geometric models
Hip_x reBOF	Coupe	60.0	22.5
	Sedan	36.3	21.9
	SUV	53.8	21.2
Eye_x reBOF	Coupe	109.2	34.5
	Sedan	105.1	24.7
	SUV	124.9	33.6
Eye_z reAHP	Coupe	73.4	35.8
	Sedan	79.8	26.1
	SUV	76.2	32.4
Eye_x reHip	Coupe	69.4	23.0
	Sedan	66.3	17.6
	SUV	75.8	28.8
Eye_z reHip	Coupe	56.3	25.6
	Sedan	60.5	25.1
	SUV	69.4	31.9

Note: $RMSE$ = root mean squared error.

Chapter 5   IDENTIFICATION OF SITTING STRATEGIES

5.1. Classification of sitting strategies by cluster analysis

The sitting strategies based on the driving postures were identified in three steps (selection of the proper number of clusters, classification of sitting strategies, and identification of sitting strategies). First, the proper number of clusters for extracted driving postures (6 joint angles) from RAMSIS was selected by dendrogram analysis of Ward's method (Figure 5.1). Second, the sitting strategies of 40 drivers' driving postures in 3 OPL conditions (120 driving postures) were statistically classified by K-means cluster analysis using the selected proper number of clusters. Lastly, the characteristics of classified sitting strategies were identified.
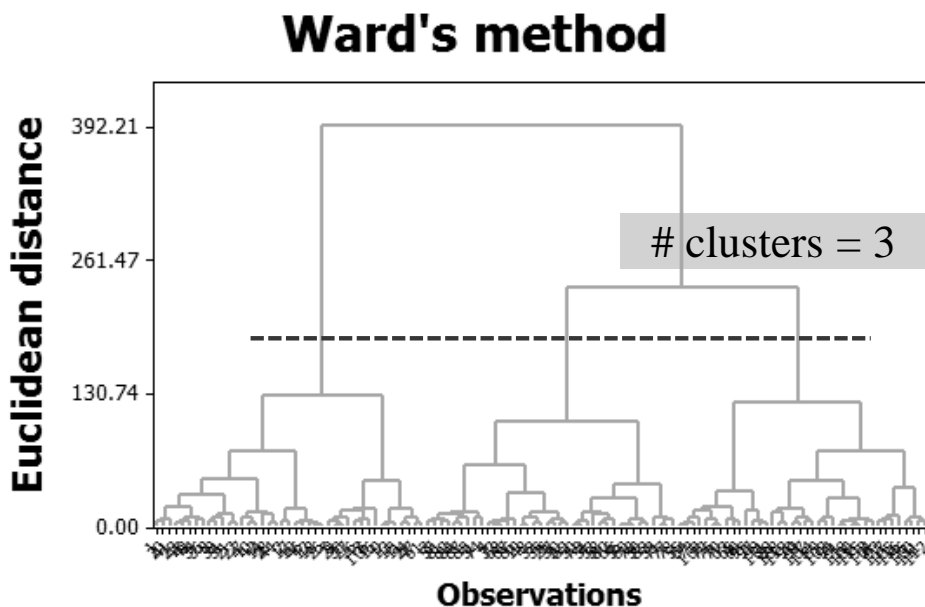
Figure 5.1. Determination of the number of clusters using dendrogram analysis

The sitting strategies for upper-body were identified as slouched, erect, and reclined posture (Figure 5.2). The sitting strategies of each upper-body were composed of 41% for slouched, 33% for erect, and 26% for reclined posture.

The sitting strategies for lower-body were identified as knee bent, knee extended, and upper-leg lifted posture (Figure 5.3). The sitting strategies of lower-body were composed of 42% for knee bent, 32% for knee extended posture, and 26% for upper-leg lifted posture.

Reclined (26%)   Slouched (41%)

25.1° ±4.7   33.6° ±5.1

6.5° ±3.4   10° ±5.2

34.8° ±4.4   23.8° ±3.2

Heal flexion   Neck flexion

Erect   Slouched   Reclined

Erect (33%)

19.3° ±5.2

17° ±4.4

30.4° ±4.9
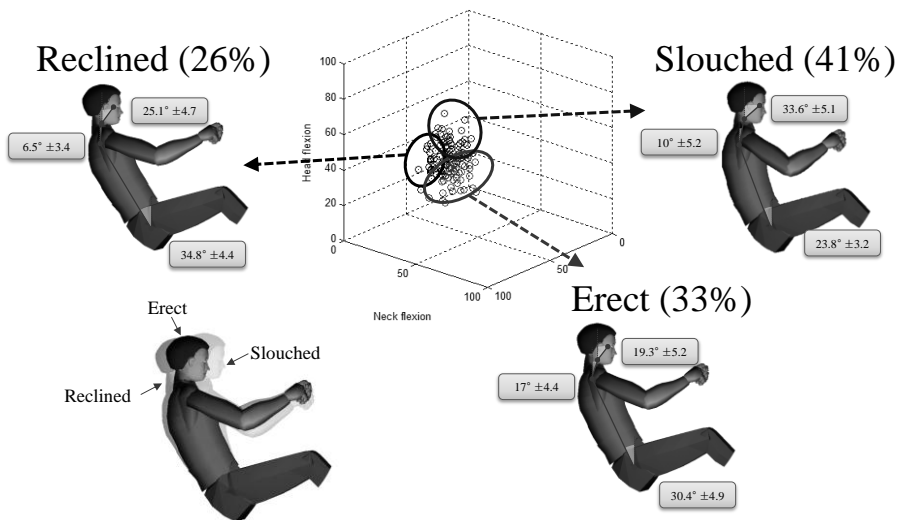
Figure 5.2. Classification of sitting strategies based of the upper-body driving posture

Knee bent (42%)   Upper-leg lifted (26%)

50.7° ±5.9   16.2° ±7.2   42.9° ±7.3

9.6° ±6.1   32.5° ±4.5

12° ±6.2

Knee extended (32%)

37.5° ±4.8

Upper-leg lifted   Knee extended   Knee bent

13.3° ±6.2   19.3° ±6.1
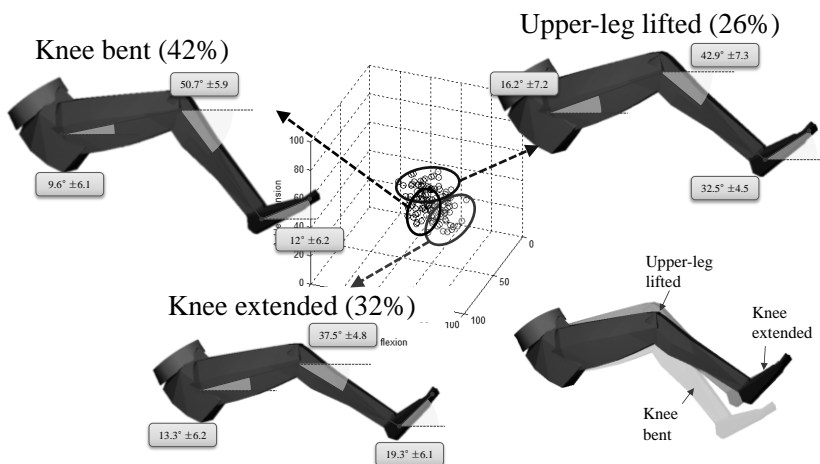
Figure 5.3. Classification of sitting strategies of the lower-body driving posture

5.2. **Identification of gender effect to the sitting strategies**

Driver's gender had significant effect on the upper-body sitting strategies ($\chi^2(2) = 8.0$, $p < .05$). As shown in Figure 5.4, 42.4% of female participants preferred erect posture; however, only 24.1% of male participants preferred erect posture. Moreover, 36.2% of male participants preferred reclined posture; however, only 15.3% of female participants preferred reclined posture. Meanwhile, As shown in Figure 5.5, there is no significance gender difference on lower-body sitting strategies ($\chi^2(2) = 3.1$, $p = .21$).
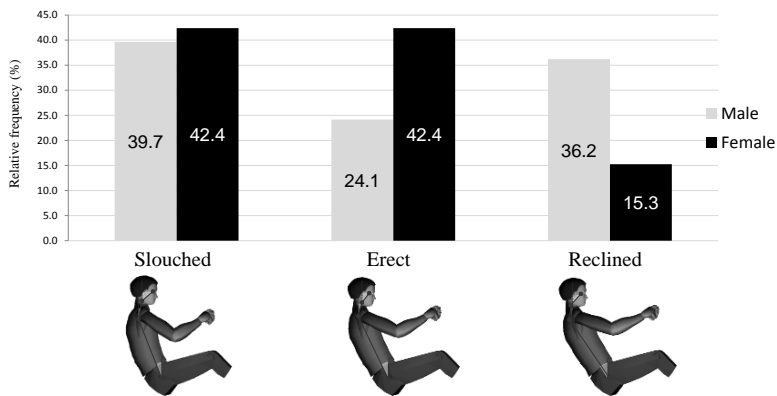
Figure 5.4. Relative frequencies of upper-body sitting strategies by gender

($\chi^2(2) = 8.0$, $p = .02$)
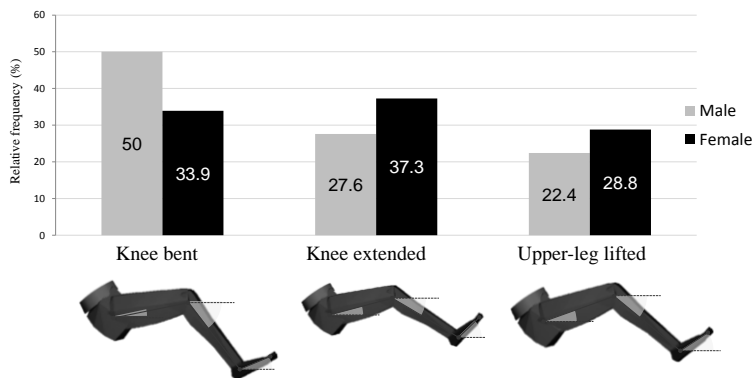
Figure 5.5. Relative frequencies of lower-body sitting strategies by gender

($\chi^2(2) = 3.1$, $p = .21$)

5.3. **Identification of OPL effect to the sitting strategies**

The OPL condition had significant effect on lower-body sitting strategies ($\chi^2(4) = 56.3$, $p < .05$). As shown in Figure 5.6, 84.2% of the participants preferred knee bent posture in the SUV condition. On the other hand, only 2.6% of the participants preferred knee bent posture in the coupe condition. Meanwhile, As shown in Figure 5.7, there is no significance OPL difference on upper-body sitting strategies ($\chi^2(4) = 2.4$, $p = .66$).
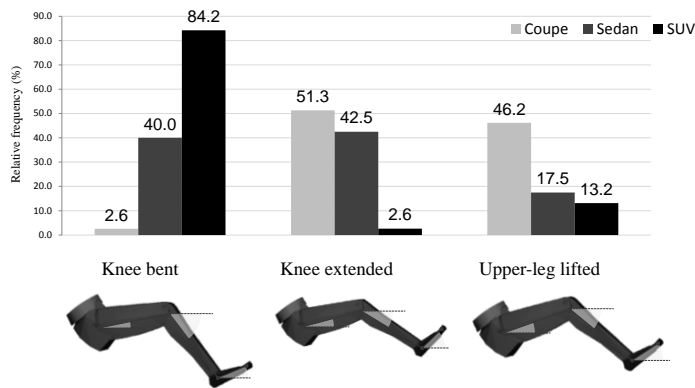
Figure 5.6. Relative frequencies of lower-body sitting strategies by OPL conditions

($\chi^2(4) = 56.3$, $p < .01$)
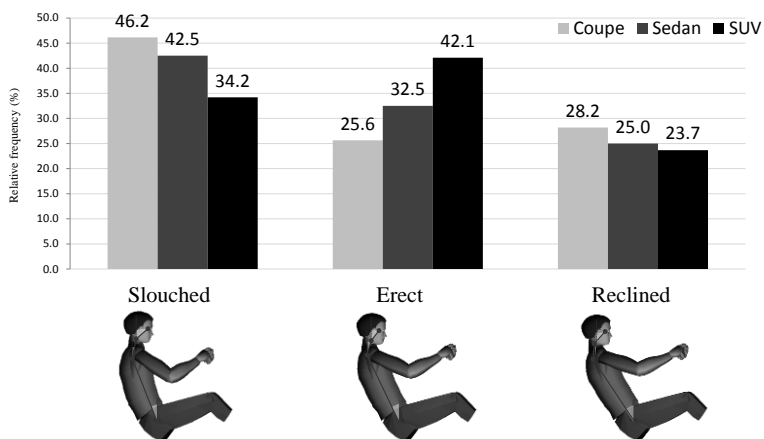
Figure 5.7. Relative frequencies of lower-body sitting strategies by OPL conditions

($\chi^2(4) = 2.4$, $p = .66$)

Chapter 6   VALIDATION OF THE SITTING STRATEGIES

6.1. Development of a measurement protocol for a field based driving posture

To validate the lab test based sitting strategies, the present study measured 214 drivers' field driving postures and applied identified lab based sitting strategies to the field observations.

The field based driving postures were measured by 3 steps (Figure 6.1). First, development of measurement protocol for driving posture step, digital single lens reflex (DSLR) camera (EOS 5D mark-2, Canon Inc., Japan) was installed on a tripod which can be used to measure a driver's whole-body driving posture at once at a side view. At this time, the driver's car door was fully opened, and the camera was located right next to the opened door (Figure 6.2).

Second, measurement of driving posture step, the present study measured 214 drivers' field driving postures. The proper sample size was determined by statistical analysis. As show in Table 6.1, the minimum sample size for field driving posture measurement was calculated by Equation 6.1 (Montgometry and Runger, 2003) using the lab based driving posture data (head, neck, and trunk angles). By considering an acceptable sampling error from the mean neck angle (11.5°), the present study determined 111 drivers for validation study as a minimum sample size at 10% of precision level (k). However, to increase the statistical power of the validation study, the present study measured 214 drivers (15 drivers and Male: Female = 12:3 for coupe; 121 drivers and Male: Female = 64:56 for sedan; 78 drivers and Male: Female = 41:37 for SUV). The participants' average ages were 40 (SD = 12.8, R = 20 ~ 77) for males and 45 (SD = 11.5, R = 20 ~ 76) for females. At the field based measurement, the participant was asked to hold 3-to-9 steering wheel positions and put his/her right foot on an accelerator pedal. Meanwhile, as shown in Figure 6.3, the measured image of driving posture has barrel distortion due to the inherence shape of circle lens. To correct the barrel distortion, image correction program (Adobe Photoshop CS 5.1, Adobe Systems Inc., USA) was used.

Third, extraction of driving posture step, the present study developed posture extraction program by Matlab® (MathWorks, Inc., USA) to extract the participant's driving posture from a measured image. Once an analyst click joint locations (eye, atlanto-occipital, C7/T1 disc center, and hip joint which were used in RAMSIS humanoid kinematic model) on the measured image using computer mouse, the program automatically calculates related segment joint angles (head, neck, and trunk angles). After measurement, the field based driving postures were classified by cluster analysis and OPL condition and gender effects were analyzed statistically. Lastly, the lab test based sitting strategy information was applied the field driving postures to classify into 3 identified sitting strategies (slouched, erect, and reclined postures) for cross validation.
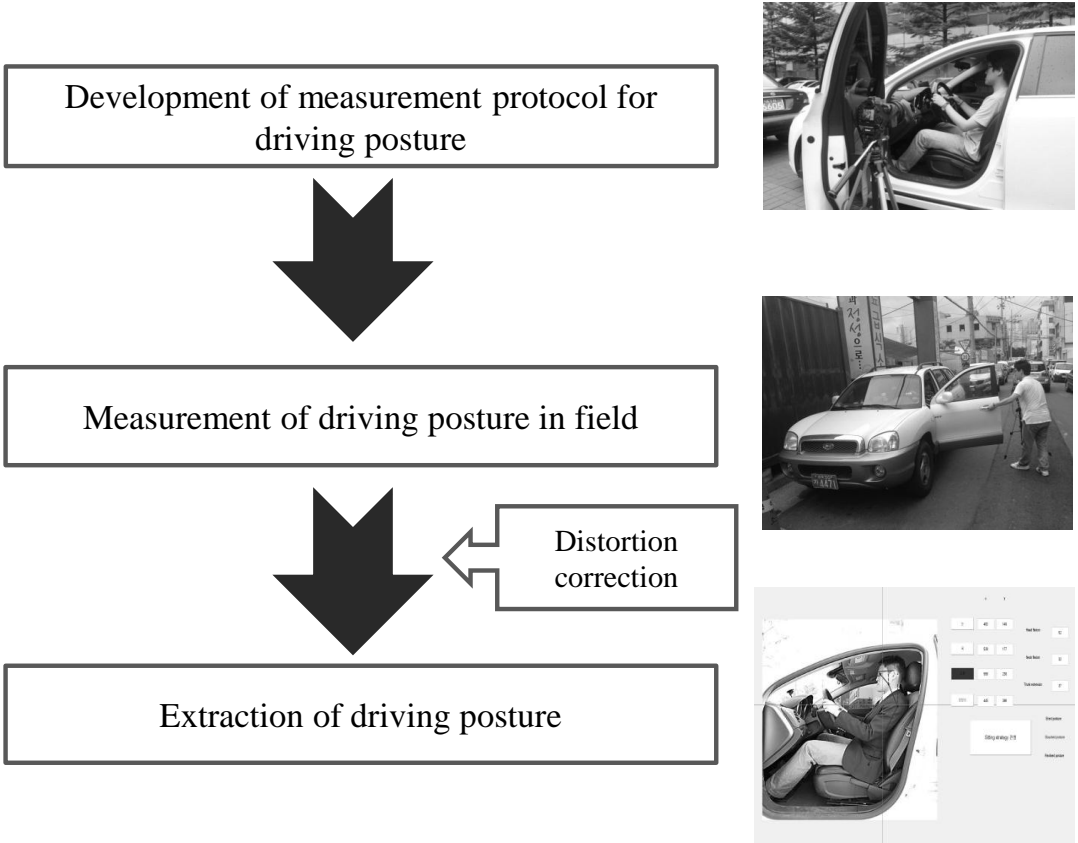
Figure 6.1. Database construction process of field based driving postures

Table 6.1. Prediction of proper sample size

Joint angle	Mean	SD	Sample size (n)					
			$k = 0.01$	$k = 0.02$	$k = 0.03$	$k = 0.04$	$k = 0.05$	$k = 0.10$
Head angle	26.6	8.0	3431	858	381	214	137	34
Neck angle	11.5	6.2	11039	2760	1227	690	442	110
Trunk angle	28.8	6.1	1720	430	191	108	69	17

$$n = (z_{\alpha/2} \times \frac{s}{k \times \bar{x}})^2$$

Equation 6.1

where: n = sample size,

z = standard normal score,

α = significant level,

s = sample standard deviation,

k = precision level,

$\bar{x}$ = sample mean

Figure 6.2. DSLR camera set-up to measure a whole-body driving posture

Figure 6.3. Image correction from barrel distortion
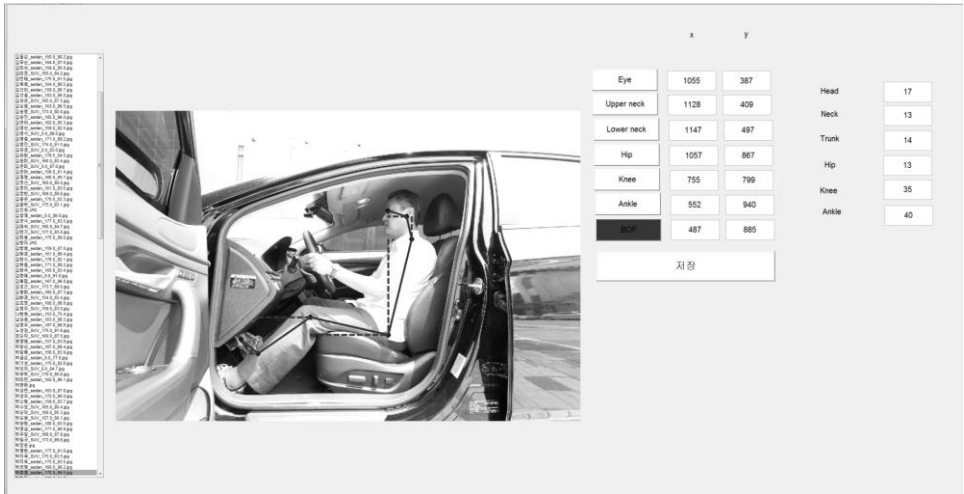
Figure 6.4. Driving posture extraction program from a measured posture image

6.2. **Identification of OPL & gender effect to the field based sitting strategies**

Identified upper-body sitting strategies based on the field observations have significant difference by OPL condition and a driver's gender. For example, as shown in Table 6.2, the OPL condition significantly affects to the upper-body sitting strategies ($\chi^2(4)$ = 51.98, p < .01); especially, in coupe condition, 73.0% of drivers preferred reclined posture and only 27.0% of drivers preferred erect posture. On the other hand, in sedan and SUV conditions, more than 40% of drivers preferred erect posture (sedan: 41.3%, SUV: 55.1%) due to a higher seat height than the coupe condition.

Meanwhile, a driver's gender significantly affects to the upper-body sitting strategies. As a result of comparison between 117 males and 107 females upper-body sitting strategies, 51.3% of male drivers (n = 60) preferred erect posture; however, only 38.1% of female drivers (n = 37) preferred erect posture (Table 6.3). Moreover, 46.4% of female drivers preferred slouched posture; however, only 29.9% of male drivers preferred slouched posture. This result indicates that the gender effect of upper-body sitting strategies which was identified in the lab test is valid.

Table 6.2. Dominant sitting strategies of OPL conditions in field
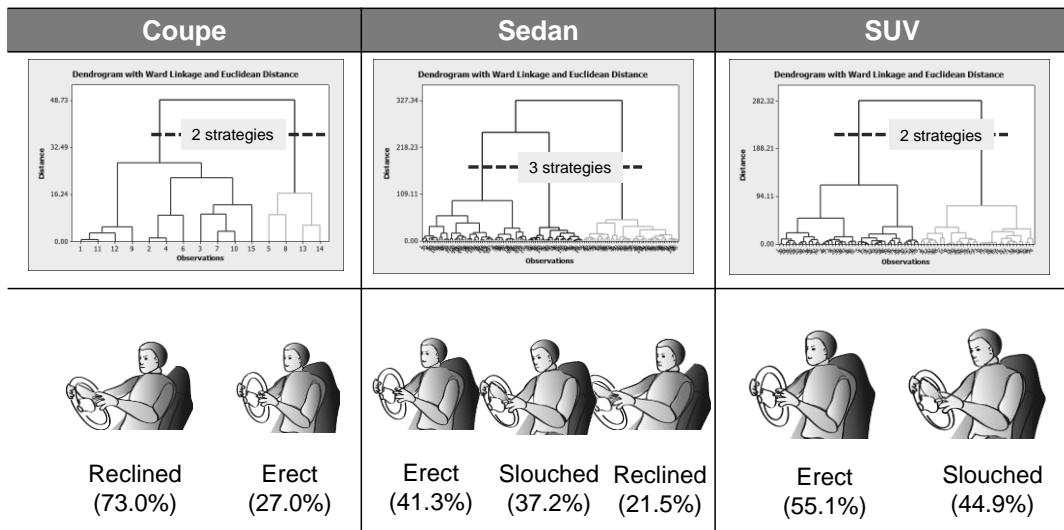
Table 6.3. Sitting strategy distribution by a driver's gender in field

Frequency (%)	Slouched	Erect	Reclined
Male	29.9%	51.3%	18.8%
Female	46.4%	38.1%	15.5%

6.3. **Cross validation of the lab based sitting strategies**

The identified lab based sitting strategies were applied to the field based driving postures to validate the lab based sitting strategies. The 187 field postures were selected for in different OPL condition (12 males for coupe, 50 males and 50 females for sedan, 35 males and 35 females for SUV) and the male-female ratio was equal for fair comparison of lab and field results (no female drivers in coupe were selected because the number of female driving postures in field was small; $n = 3$). As a result of comparison, lab and field based sitting strategies shows similar distribution trend in different OPL conditions (Figure 6.5) and there is no significant differences of their homogeneity between the lab and field based sitting strategies ($p = 39$ for coupe, $p = .78$ for sedan, and $p = .37$ for SUV).
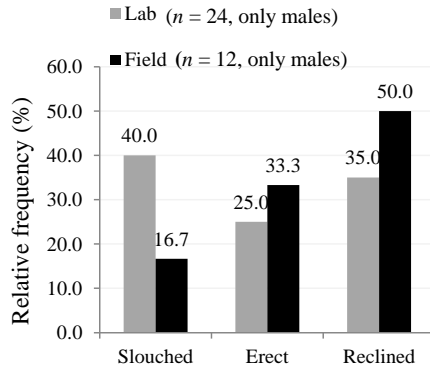
(a) Coupe condition: $\chi^2(2) = 1.91$, p = .39
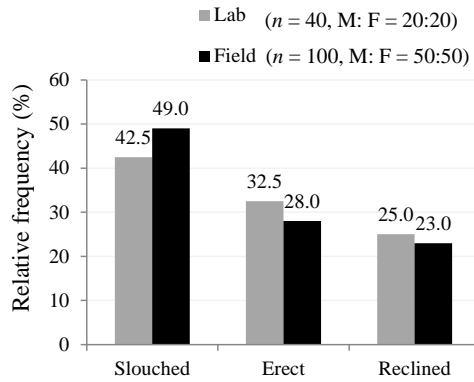
(b) Sedan condition: $\chi^2(2) = 0.50$, p = .78
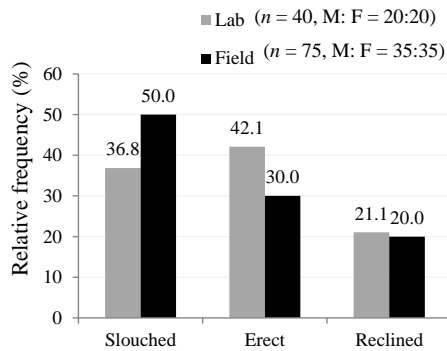
(c) SUV condition: $\chi^2(2) = 2.01$, p = .37

Figure 6.5. Distributions of lab and field based sitting strategies

Chapter 7   DISCUSSION

7.1. **Statistical geometric models**

The present study measured the HLs, ELs and driving postures of drivers who have various body sizes with three OPL conditions (coupe, sedan, and SUV) using a seating buck, a motion capture system, and RAMSIS[®]. The seating buck has characteristics to represent various OPL conditions by adjusting a steering wheel, pedals, and the seat location. Also, the motion capture system (Motion Analysis Co., USA) can accurately measure (measurement error < 0.5 mm) the markers (ø = 1.2 cm) attached to the whole-body of the participants, therefore more an accurate posture measurement can be made than an image based posture measurement method (Na et al., 2005). The present study synchronized the marker data measured by a motion capture system with reference points on a RAMSIS humanoid, the participants' HLs and ELs were extracted more accurately and systematically.

The developed SGMs show more predominant prediction accuracy and stability than the Reed et al.'s models. Adj. R^2s of the SGMs are 1.1 ~ 3.7 times higher than the Reed et al.'s models in average and *RMSE* of the SGMs are 1.7 ~ 1.8 times smaller than the Reed et al.'s models. Moreover, the *RMSE* of the SGMs are 1.7 ~ 4.3 times smaller than the Reed et al.'s models for different OPL conditions (coupe, sedan, SUV). As a result of the performance evaluation of the SGMs, the SGMs have better prediction accuracy than the Reed et al.'s models because of a small variation of prediction errors. Additionally, the SGMs have better prediction stability because the SGMs show a small variation of *RMSE* for the different OPL conditions (*RMSE* range is 36.3 mm ~ 124.9 mm for the Reed et al.'s models and 17.6 mm ~ 35.8 mm for the SGMs).

The SGMs are consists of both geometric equations and statistical coefficients, so that the SGMs effectively overcome the limitations (low prediction accuracy, hard to measure a link length) of previous geometric models and statistical models. According to the study of ANSI/HFES 100 (2007), Diffrient et al. (1981), Jung et al. (2010), and You et al. (1997),

drivers or pilots' HL and EL can be predicted by a geometric equation which consists of related body link lengths and joint angles. However, the driver's or pilot's link lengths cannot be measured precisely in real because the link length is an anatomical length, not a measurable length. Generally, an anthropometric dimension of a driver can be easily measured by surface landmark length which is the distance between two landmarks on the driver's skin (Chaffin et al., 2006) and there is an official measurement protocol such as the Size Korea anthropometry. However, the femoral link and shank link lengths of Diffrient et al.'s model cannot be accurately measured by a general anthropometer. On the other hand, the SGMs used statistically identified link length conversion ratios, so that the SGMs are applicable to predict a driver's HL and EL using surface measurement lengths.

Two types of error may occur when synchronizing the measured driving posture to the digital humanoid of RAMSIS. First, the position differences between the reference points and markers attached on body may cause an error. To reduce the error of position differences, the reference points were defined an anatomical landmark marker attached on the body and the reference points of the humanoid were manually corrected according to the distance from the measured markers. Second, skin deformation from body movement may affect the mapping quality of the markers to the reference points because it can change the positions of the markers. Ryu (2006) reported marker displacement due to skin deformation during walking, and Cappozzo et al. (1996) reported that the marker positions attached to thigh and shank can vary 10 ~ 40 mm depending on gait motions. However, the RAMSIS humanoid does not have a reference point correction function due to skin deformation. Therefore, to generate more accurate postures from motion data in RAMSIS, reference point correction should be applied.

7.2. **Sitting strategies**

The identified sitting strategies of the present study are more objective and reliable than the existing sitting strategies. The Andreoni et al. (2002)'s sitting strategy classification method was insufficient because they classified the sitting strategies with an

analyst's visual observation of seating pressure distribution. However, the present study's used quantitative posture data and the classification method was cluster analysis. Therefore, the identified sitting strategies of the present study are more objective and reliable than the Andreoni et al.'s sitting strategies.

A driver's gender significantly effects on the upper-body sitting strategies. The present study identified that male drivers preferred the slouched and reclined posture (percentage of slouched posture = 39.7%, erect posture = 24.1%, and reclined posture = 36.2%); however, female drivers preferred the slouched and erect posture (percentage of slouched posture = 42.4%, erect posture = 42.4%, and reclined posture = 15.3%). This result indicates that since the arm-length of female drivers is relatively shorter than that of males, female drivers moved their upper-body toward to the steering wheel to grasp the steering wheel appropriately. Also, since the sitting height of females is relatively shorter than that of males, female drivers might have moved their upper-body toward to the steering wheel to secure enough view angles. Meanwhile, the difference of preferred driving postures depending on the gender could be used as representative driving postures of female and male digital human models of automobile interior design process. For example, by selecting slouched posture and erect posture as representative postures for a female humanoid, the evaluation of an automobile interior design can be effectively performed.

OPL condition significantly effects on lower-body sitting strategies. In this study, 84.2% of the participants preferred knee bent posture in the SUV condition; on the other hand, only 2.6% of the participants preferred knee bent posture in the coupe condition. This result indicates that driver's lower-body posture is affected by a seat height (H30). For example, SUV condition (seat height = 305 mm), since the height of seat position from the floor was higher than other OPL conditions (e.g., coupe, sedan), drivers pulled their seat position toward to the pedal and bend their knees to control the pedal comfortably. On the other hand, in coupe condition (seat height = 176 mm), since the seat height is lower than other OPL conditions (e.g., sedan, SUV); therefore, the drivers might have moved the seat to the backward direction and made the knee extended posture to control the pedal

comfortably. This result also can be used in a digital human model; for example, by selecting knee bent posture as the representative posture for lower-body of humanoid in SUV type automobile design and evaluation.

The identified sitting strategies in lab and their characteristics were validated by the comparison of field driving postures. A driver's gender is a significant factor to strongly effect the portion of upper-body sitting strategies in field ($\chi^2(2) = 6.21$, $p = 0.05$); and also OPL condition can be one of the significant factors to affect upper-body sitting strategies in field ($\chi^2(4) = 51.98$, $p < .01$). As a result of cross validation, the identified slouched, erect, and reclined postures in lab test were valid in field driving postures. This result indicates that the identified sitting strategies in the lab test were valid in a field based driving posture.

Lastly, the identified sitting strategies and proposed SGMs of the present study can be effectively used to design/evaluate a car seat design. The effective and efficient ergonomics evaluation of a car seat using the DHMS system is significantly affected by the hip and eye location of representative digital human models (5th, 50th, and 95th %ile) and their sitting strategies (slouched, erect, and reclined posture). Therefore, if the proposed SGMs and sitting strategies are synchronized with existing DHMS systems (RAMSIS, Safework®, and Jack®) then they will be an useful design support tool of an automobile interior.

7.3. **Application: identification of sitting strategy based eyellipses**

The identified sitting strategies and developed SGMs can be used to predict Korean drivers' eyellipses in their preferred driving posture strategies. Although SAE proposed the various sizes of US drivers' eyellipses by considering various coverage percentages, these are hard to apply for Korean drivers due to anthropometric differences between US drivers and Korean drivers. However, the identified 3 upper-body sitting strategies of Korean drivers and SGMs can be effectively synchronized to predict the eyellipses for each sitting

strategies. Therefore, the sitting strategy based eyellipses will be useful reference data to design an automobile interior by considering Korean drivers' preferred driving postures.

Meanwhile, the present study predicted the Korean drivers' eyellipses based on the identified sitting strategies and developed SGMs, and compared the sitting strategy based eyellipses and SAE eyellipses in different OPL conditions. As a result of comparison, sizes and centroid locations of eyellipses were different. For example, x-axis lengths of SAE eyellipses are same (206 mm) for all OPL conditions (coupe, sedan, and SUV); however, the x-axis lengths of reclined sitting strategies are different for all OPL conditions (152 mm for coupe, 164 mm for sedan, and 250 mm for SUV). Moreover, the centroid locations of sitting strategy based eyellipses were located 110 mm forward and 60 mm downward from those of SAE eyellipses in average. These differences between SAE eyellipses and sitting strategy based eyellipses are explained by following three reasons; First, seatback angle might be fixed at the SAE experimental condition; however, in the present study, seatback angle was adjustable by the participant's preferred position. Second, anthropometric differences between US drivers and Korean drivers may affect. Lastly, in the present study, there is no roof condition on the seating buck; however, in the SAE experimental condition, the visibility of participant might be restricted by certain package condition to generalize a field driving circumstance. In conclusion, the sitting strategy based eyellipses can be applied to design an automobile package layout for Korean drivers.

Table 7.1. Design specifications of eyellipses for each sitting strategies

| Eyellipse	OPL condition	Centroid location (mm)		Eyellipse size (mm)		Tilted angle (°)
		x	z	x-axis length	z-axis length	
SAE (95% tangent cutoff)	Coupe	967	841	206	94	2.7
	Sedan	943	905	206	94	3.8
	SUV	913	970	206	94	4.7
Reclined sitting	Coupe	881	762	152	110	17
	Sedan	880	815	164	146	7.2
	SUV	860	884	250	210	20.8
Erect sitting	Coupe	832	820	224	216	-1.5
	Sedan	811	851	224	166	11.9
	SUV	769	903	288	234	15
Slouched sitting	Coupe	830	802	168	146	1.5
	Sedan	831	872	206	188	10.4
	SUV	771	925	288	198	15.1
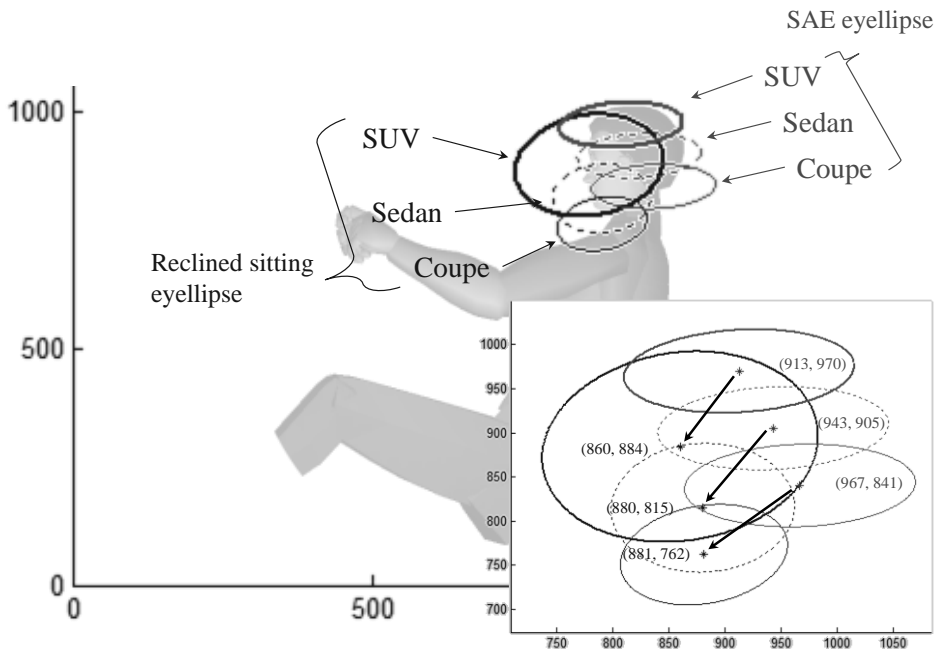
Figure 7.1. SAE 95% tangent cutoff eyellipses vs. reclined sitting eyellipses
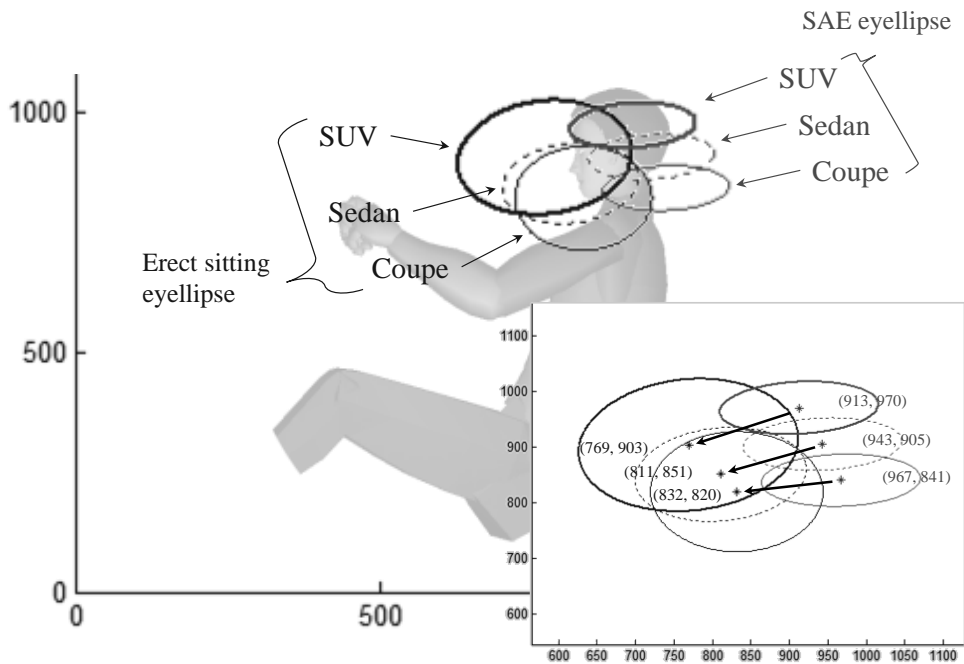
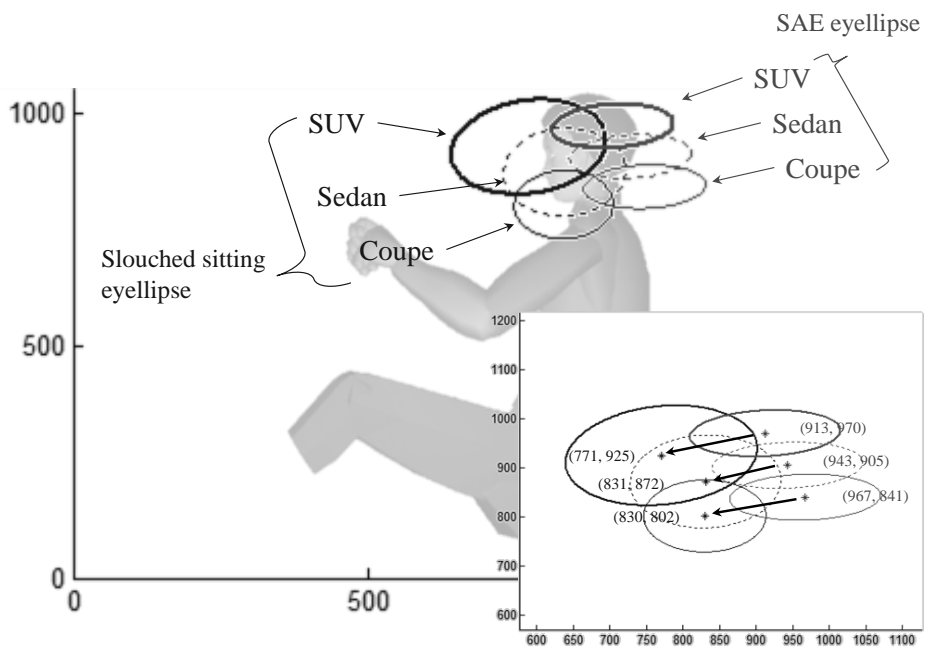Figure 7.2. SAE 95% tangent cutoff eyellipses vs. erect sitting eyellipses

Figure 7.3. SAE 95% tangent cutoff eyellipses vs. slouched sitting eyellipses

Chapter 8   CONCLUSION

The present study has three contributions. First, the present study developed the statistical geometric models (SGMs) using 40 drivers' HLs and ELs, anthropometric dimensions, driving postures and the prediction performance of the SGMs were evaluated by comparing with Reed et al.'s HL and EL models. Regression equations were constructed based on the geometric equations to consider the conversion relationships between the link lengths and the corresponding surface landmark lengths (buttock-popliteal length, knee height, and foot length). Lastly, the SGMs were compared with Reed et al.'s HL and EL models in terms of adj. R^2 and $RMSE$. The SGMs are compared to Reed et al.'s models in aspect of prediction accuracy (adj. R^2, root mean squared error) and stability (root mean squared error for OPL conditions). SGMs have higher design applicability than Reed et al.'s models due to higher prediction accuracy and stability. The SGMs produce a higher prediction accuracy (range of adj. $R^2 = 0.23 \sim 0.89$ for Reed et al.'s models and $0.69 \sim 0.85$ for SGMs; range of $RMSE = 21.8$ mm ~ 50.9 mm for Reed et al.'s models and 21.1mm $\sim$ 29.9 mm for SGMs) and fewer accuracy variables for different OPL types as a result of higher stability (range of $RMSE = 36.3$ mm ~ 124.9 mm for Reed et al.'s models and 17.6 mm ~ 35.8 mm for SGMs) than Reed et al.'s models.

Second, the sitting strategies of driving postures and factors to affect the sitting strategies were quantitatively identified. Andreoni et al. (2002)'s sitting strategy classification method was insufficient because sitting strategies were subjectively classified by an analyst's visual observation of seating pressure distribution. Although, Park (2006) identified 5 sitting strategies through cluster analysis based on 126 Korean male drivers' driving posture data, the factors (driver's gender, OPL condition) to affect the sitting strategies were not analyzed clearly. However, the present study's classification method is more objective than previous research due to quantitative posture data and K-means cluster analysis method. Moreover, the present study identified a driver's gender and OPL condition effect to the classified sitting strategies in a statistical manner.

Lastly, the identified sitting strategies were validated by field based driving postures. The present study developed field based driving posture measurement protocol using driving posture images. Two hundred fourteen drivers' driving posture images were measured and upper-body driving postures (head, neck, and trunk angles) were extracted by Matlab coding. Next, the identified sitting strategies in lab test were applied to the field based driving postures and the distributions of sitting strategies in different OPL conditions were compared. As a result, the frequencies of sitting strategies in OPL conditions show no significant differences the homogeneity between lab based and field based sitting strategies.

As a future study, the proposed SGMs and sitting strategies can be applied to design/evaluate an automobile seat design using digital human model simulation (DHMS) and occupant package tool such as eyellipse. The effective and efficient ergonomics evaluation of an automobile seat using the DHMS system is available based on the hip and eye location of representative digital human models (5th, 50th, and 95th %ile) and their sitting strategies (slouched, erect, and reclined posture). Next, identified sitting strategies and developed SGMs are used to generate the eyellipses, and these eyellipses of sitting strategies are applicable to design a package layout such as windshield height, rearview mirror size, and pillar size, etc.

요약문

운전자의 hip locations (HLs)과 eye locations (ELs), 그리고 sitting strategies는 차량 운전석의 인간공학적 설계 측면에서 중요 참조자료로 활용되고 있다. HL은 운전자의 엉덩이 위치를 나타내는 좌표로서 운전자들의 HL 위치 분포는 운전석의 적정 조절범위 설계에 중요 참조 자료로 활용되고 있으며, EL은 운전자의 눈 위치를 나타내는 좌표로서 다양한 인체크기를 가진 운전자들의 운전자세로부터 수집되며, 수집된 EL 분포(eyellipse)는 운전석의 visibility 평가에 중요 도구로 활용되고 있다. 또한, sitting strategy는 운전자들이 선호 운전자세 유형으로서 3D 가상환경 기반의 차량 설계/평가 시 인체모델이 취하는 운전자세 설정에 참조 자료로 활용될 수 있다.

　　Occupant package layout (OPL)의 인간공학적 설계를 위해 운전자의 hip & eye location을 추정할 수 있는 통계적 모형들이 개발되었으나 기존 개발된 모형들은 추정 정확성 측면에서 한계가 있었다. 또한, 가상환경에서의 차량 운전석 설계 평가 시 인체모델의 운전 자세 생성을 위한 운전자들의 자세 정보가 필요하나 기존 연구는 운전자들의 sitting strategy를 파악하는 단계에만 그쳤을 뿐 운전자의 성별이나 OPL 조건이 sitting strategy에 미치는 영향을 분석하지는 않았다.

　　본 연구는 (1) 운전자들의 인체크기 및 운전자세를 기반으로 운전자의 HL과 EL을 추정할 수 있는 statistical geometric models (SGMs)를 개발하고 그 효과를 평가, (2) 운전자들의 다양한 자세 유형을 통계적으로 적합하게 대표하는 sitting strategies 파악 및 연관 인자 분석, 마지막으로 (3) 파악된 sitting strategies를 실차 운전자세 data를 바탕으로 검증하는 것이다.

　　본 연구는 40명의 남녀 운전자들을 대상으로 coupe, sedan, SUV package 조건에서 motion capture system을 이용해 운전자들의 자세를 측정하였다. 측정된 운전자세는 인체모델와 연동되어 RAMSIS®의 3D 가상환경에서 재현되었으며,

인체모델로 재현된 실험 참여자들의 운전자세로부터 관절각도 및 HL과 EL 정보가 추출되었다. SGMs는 운전자들의 인체크기, 관절각도, 그리고 HL과 EL 간의 기하학적 연관식에 통계적 보정과정을 거쳐 개발되었으며, sitting strategies는 운전자세의 군집분석을 통해 파악되었다.

개발된 SGMs는 기존 개발된 HL과 EL 추정식들에 비해 추정 정확성이 우수하여 실무에서 유용하게 활용될 수 있을 것으로 기대된다. SGMs는 Reed et al. (2002)의 모형들에 비해 adj. R^2가 1.1 ~ 3.7배 높은 것으로 나타났으며 오차($RMSE$)는 1.7 ~ 1.8배 작은 것으로 파악되었다. 또한, 개발된 SGMs를 다양한 OPL 조건(coupe, sedan, SUV)에서 HL과 EL 추정에 적용했을 때 SGMs는 Reed et al.의 추정 모형들에 비해 RMSE가 1.7 ~ 4.3배 작아 추정 안정성이 우수한 것으로 나타났다. 개발된 SGMs는 기존 Reed et al.의 추정 모형들에 비해 추정 정확성이 향상되었을 뿐만 아니라 다양한 OPL 조건에 적용 시 추정 안정성이 우수해 차량 설계 평가 시 높은 활용성이 기대된다.

운전자들의 sitting strategies는 통계적 분석을 거쳐 상체 3가지 유형(slouched erect, 그리고 reclined posture)과 하체 3가지 유형(knee bent, knee extended, 그리고 upper-leg lifted)으로 분류되었다. 분류된 상체 sitting strategies는 OPL 조건에는 영향을 받지 않는 것으로 나타났으나 운전자의 성별에 따라서는 선호하는 sitting strategies의 비중에서 유의한 차이가 있는 것으로 나타났다. 예를 들어, 남성의 경우 36%가 reclined posture를 선호하는 반면 여성의 경우는 15%만이 선호하였다. 반면, erect posture에서는 남성이 24.1%로 여성 42.4%에 비해 절반 가량으로 나타났다. 반면 하체 sitting strategies는 운전자의 성별에는 영향을 받지 않았으나 OPL 조건에 따라 유의하게 바뀌는 것으로 나타났다. 예를 들어, knee bent 유형은 84%가 SUV 조건에서 취하는 반면, knee extended 유형의 51%는 coupe 조건에서 취하는 것으로 나타났다.

한편, 기 분류된 sitting strategies는 field test를 기반으로 한 운전자세를 바탕으로 검증되었다. 본 연구는 운전자세 사진으로부터 정량적인 자세

정보(관절 각도)를 추출할 수 있는 protocol을 고안함으로써 214명(남성: 117명, 여성: 107명)의 운전자세를 촬영하고 개발된 protocol에 따라 추출된 운전자세 정보를 DB화 하였다. 사진 분석을 통해 수집된 운전자세들을 lab test를 통해 기분류된 sitting strategy에 적용해본 결과, OPL 조건별 상체 sitting strategy 분포 경향이 lab test 결과와 field test 결과 간에 통계적으로 유의한 차이가 없는 것으로 나타났다(coupe 조건: p = .39, sedan 조건: p = .78, 그리고 SUV 조건: p = .37).

　　본 연구에서 개발된 SGMs와 파악된 sitting strategies는 digital human model simulation (DHMS)의 인체모델과 연계 활용, 또는 차량 운전석 설계를 위한 중요 참조 도구(예: eyellipse) 생성에도 활용될 수 있다. Sitting strategy와 SGMs의 연계 활용은 차량 운전석 조절범위 설계, windshield의 높낮이 설계, package 공간의 component 배치 등 차량 운전석 설계 전반에서 효과적으로 적용될 것으로 기대된다.

REFERENCES

Andreoni, G., Santambrogio, G. C., Rabuffetti, M., & Pedotti, A. (2002). Method for the analysis of posture and interface pressure of car drivers. *Applied Ergonomics*, *33*, 511-522.

ANSI/HFES 100 (2007). *Human Factors Engineering of Computer Workstations*. Santa Monica, CA: Human Factors and Ergonomics Society.

Bhise, V. (2011). *Ergonomics in the automotive design process*. Boca Raton, FL: CRC Press.

Bittner (2000). A-Cadre: advanced family of manikins for workstation design, *Proceeding of the Human Factors and Ergonomics Society*.

Cappozzo, A., Catani, F., Leardini, A., Benedetti, M. G., & Della Croce, U. (1996). Position and orientation in space of bones during movement: Experimental artifacts. *Clinical Biomechanics, 11*(2), 90-100.

Chaffin, D. B., Andersson, G. B. J., and Martin, B. J. (2006). *Occupational Biomechanics* (4th ed). New York, USA: Wiley Interscience.

Chaffin, D. B. (2001). *Digital Human Modeling for Vehicle and Workplace Design*. Society of Automotive Engineers, Warrendale, Pa: SAE International.

Choi, Y. (2012). *Sitting Strategy Analysis based on Driving Posture and Seating Pressure Distribution* (Unpublished master's thesis), POSTECH, Pohang, South Korea.

Department of Defense Design Criteria Standard. *Human Engineering* (MIL-STD-1472F), Washington, 1999.

Diffrient, N., Tilley, A. R. & Harman, D. (1981). *Human Scale 7/8/9*, Cambridge, MA.

Edsall, L. (2004). Mitsubishi outlander new car test drive. Retrieved February 14, 2011, from http://www.buybob.com/reviews/2004/mitsubishi/outlander.

Gordon, C. C., Bradtmiller, B., Churchill, Y., Clauser, C. E., McConville, J. T., Tebbetts, I. O., and Walker, R. A. (1988). *1988 Anthropometric Survey of U.S. ARMY Personnel: Methods and Summary Statistics* (Technical Report NATICK/TR-89/044), US Army Natick Research Center: Natick, MA.

Jang, C., & Lim, S. (2010). Current trends and future issues of automotive ergonomics. *Journal of the Ergonomics Society of Korea. 29*(1), 1-5.

Jung, K. (2009). *Development of a Multivariate Representative Human Model Generation Method for Anthropometric Design* (Unpublished doctoral dissertation), POSTECH, Pohang, South Korea.

Jung, K., Park, J., Lee, W., Kang, B., Eum, J., Park, S., and You, H. (2010). Development of a quantitative ergonomic assessment method for helicopter cockpit design in a digital environment. *Journal of the Ergonomics Society of Korea*, *29*(2), 203-210.

Kyung, G., & Nussbaum, M. A. (2009). Specifying comfortable driving postures for erfonomic design and evaluation of the driver workspace using digital human models. *Ergonomics. 52*(8), 939-953.

Lee, B. (2009). *Development of a Distributed Representative Human Model Generation and Analysis System for Multiple-Size Product Design* (Unpublished master's thesis), POSTECH, Pohang, South Korea.

Mergl, C., Klendauer, M., Mangen, C., & Bubb, H. (2005). Predicting long term riding comfort in cars by contact forces between human and seat. *SAE Technical Paper* no. 2005-01-2690.

Montgomery, D. and Runger, G. (2003). *Applied Statistics and Probability for Engineers* (3rd ed.). Hoboken, NJ: Wiley.

Na, S., Lim, S., Choi, H., & Chung, M. (2005). Evaluation of driver's discomfort and postural change using dynamic body pressure distribution. *International Journal of Industrial Ergonomics*, *35*, 1085-1096.

Park, J., Jung, K., Chang, J., Kwon, J., & You, H. (2010). Evaluation of predicted driving postures in RAMSIS digital human model simulation. *IE Interfaces*, *23*(2), 101-108.

Park, S. (2006). Estimation of driver′s standard postures by a multivariate analysis method. *Journal of the Ergonomics Society of Korea. 25*(1), 27-33.

Park, S., Kim, C., Kim, C., & Lee, J. (2000). Comfortable driving postures for Koreans. *International Journal of Industrial Ergonomics*. *26*, 489-497.

Parkinson, M., Reed, M., Kokkolars, M., & Papalambros, P. (2005). Robust truck cabin layout optimization using advanced driver variance models. *Proceeding of the ASME International Design Engineering Technical Conferences*. Long Beach, CA.

Parkinson, M., Reed, M., Kokkolars, M., & Papalambros, P. (2007). Optimizing truck cab layout for driver accommodation. *ASME Journal of Mechanical Design. 129*(11), 1110-1117.

Reed, M. P., Flannagan, C. A. C., Manary, M. A., & Schneider, L. W. (2001). *Modeling vehicle occupant head and head restraint positions*. University of Michigan Transportation Research Institute, Biosciences Dvision, Report No: UMTRI-2001-8.

Reed, M. P., Manary, M. A., Flannagan, C. A. C., & Schneider, L. W. (2000). Effects of vehicle interior geometry and anthropometric variables on automobile driving posture. *Human Factors, 42*(4), 541–552.

Reed, M. P., Manary, M. A., Flannagan, C. A. C., & Schneider, L. W. (2002). A statistical method for predicting automobile driving posture. *Human Factors, 44*(4), 557–568.

Philippart, N. L., Roe, R.W., Arnold, A. J., & Kuechenmeister, T. J. (1984). *Driver selected seat position model*. SAE Techni cal Paper 840508. Warrendale, PA: Society of Automotive Engineer Inc.

Roe, R.W. (1993). *Occupant Packaging*. In Automotive Ergonomics, ed. B. Peacock and W. Karwowski. Taylor and Francis, London.

Ryu, T. (2006). *A Direct Estimation of Anatomical Landmark Positions from Skin Markers by Identifying the Displacement Relationship* (Unpublished doctoral dissertation), POSTECH, Pohang, South Korea.

SAE J182 (2009). *Motor vehicle fiducial marks and three-dimensional reference system*. Warrendale, PA: Society of Automotive Engineers, Inc.

SAE J287 (2007). *Driver hand control reach*. Warrendale, PA: Society of Automotive Engineers, Inc.

SAE J826 (1995). *Devices for use in definning and measureing vehicel seating accommodation*. Warrendale, PA: Society of Automotive Engineers, Inc.

SAE J941 (2010). *Motor vehicle drivers' eye locations*. Warrendale, PA: Society of Automotive Engineers, Inc.

SAE J1100 (2005). *Motor vehicle dimensions*. Warrendale, PA: Society of Automotive Engineers, Inc.

SAE J1517 (2011). *Driver selected seat position*. Warrendale, PA: Society of Automotive Engineers, Inc.

SAE J4002 (2008). *H-point machine and design tool procedures and specifications*. Warrendale, PA: Society of Automotive Engineers, Inc.

SAE J4004 (2009). *Positioning the H-point design tool - seating reference point and seat track length*. Warrendale, PA: Society of Automotive Engineers, Inc.

Seo, S., Shim, J., & Choi, T. (2010). The role of ergonomics in the vehicle development stage, *Journal of the Ergonomics Society of Korea. 29*(1), 7-16.

Size Korea (2010). *Report on the Fifth Survey of Korean Anthropometry*. Retrieved June 26, 2010 from http://sizekorea.kats.go.kr/

Speyer, H. (2005). *RAMSIS Definition of Anthropometric Measurements*. Human Solutions GmbH, Germany.

You, H., Oesterling, B., Bucciaglia, J., Lowe, B. D., Gilmore, B. J. & Freivalds, A. (1997). *Bus operator workstation evaluation and design guidelines*. Transit Cooperative Research Program, National Academy Press, Washington, D.C.

You, H., Bucciaglia, J., Lowe, B. D., Gilmore, B. J., and Freivalds, A. (1997). An ergonomic design process for a US transit bus operator workstation. Heavy Vehicle Systems, A Series of the *International Journal of Vehicle Design*, 4(2-4), 91-107.

Zenk, R., Mergl, C., Hartung, J., Sabbah, O., and Bubb, H. (2006). Objectifying the comfort of car seats. *SAE Technical Paper* no. 2006-01-1299.